Three-dimensional Wave Patterns Observed at the Sea Surface

Guillemette Caulliez and Fabrice Collard

Laboratoire des Interactions Océan-Atmosphère

Institut de Recherche sur les Phénomènes Hors Equilibre - Marseille

Three-dimensional wind waves observed at sea

when wind starts to blow, well-organised 3D short wave patterns can be observed:
rhombic patterns due to two waves propagating obliquely to the wind

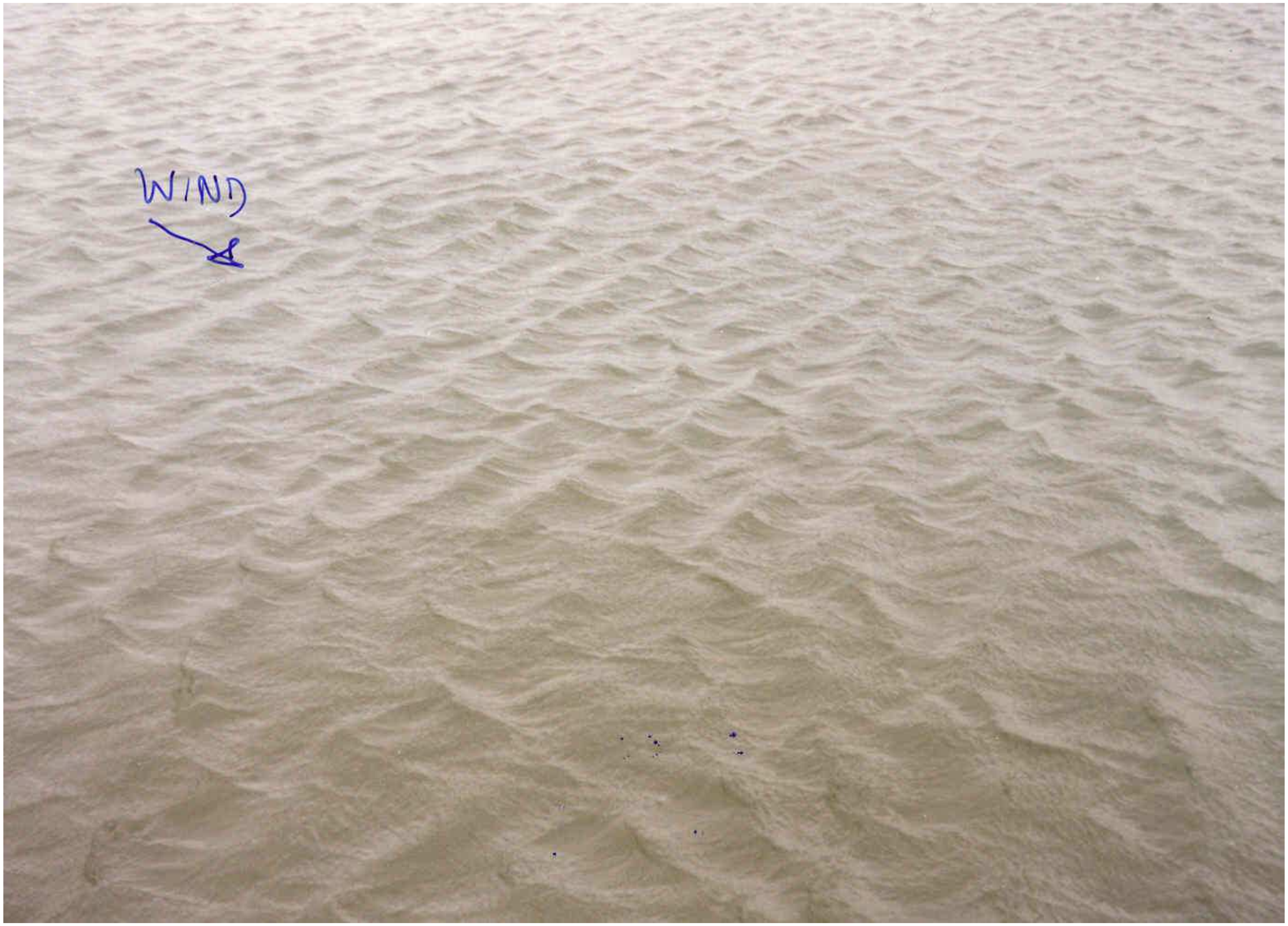

when stronger wind blows, cross-hatched wave patterns are visible
(courtesy of E. Mollo-Christensen)

when wind waves break, they exhibit a particular shape
characterized by a crescent-like or 'horse-shoe' crest

Wind wave fields are essentially three-dimensional

Various wave patterns may be identified as:

- rhombic short wave patterns,
- cross-hatched short wave patterns,
- horse-shoe near-breaking wave patterns.

Two detailed investigations were performed in laboratory:

⇒ to characterize the main features of the 3D wind wave patterns;

⇒ to determine the conditions of their emergence as function of "external" parameters as wind speed, or intrinsic wave field parameters as wavelength , wave steepness.

Motivations:

- to better understand and modelize the radar signature of the sea surface;
- to identify the basic nonlinear processes leading to the 3D wave pattern formation.

Experimental procedure

The large IRPHE-Luminy wind wave facility

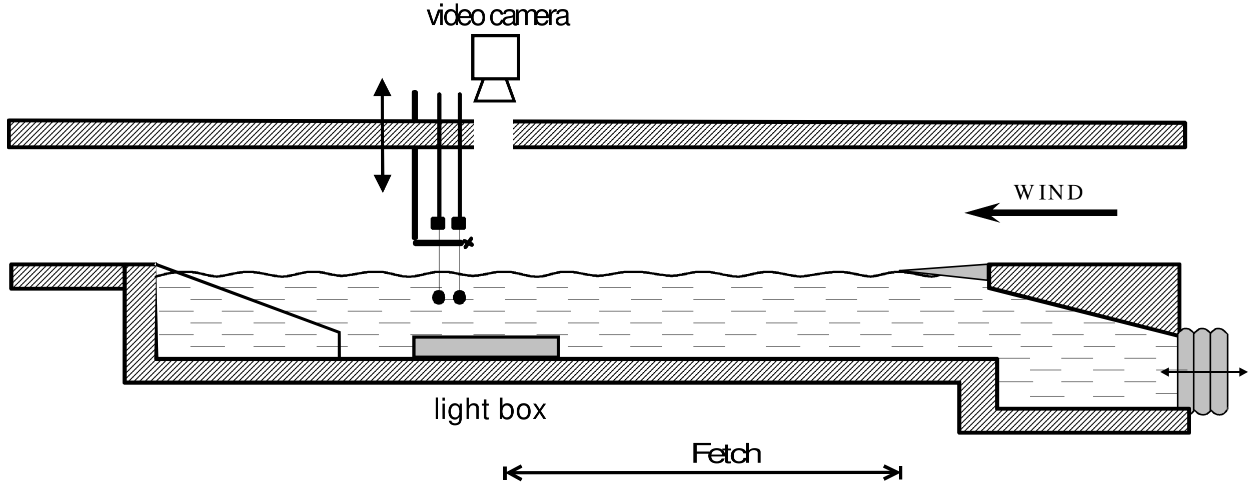

length : L = 40 m ; width : l = 2.6 m ;
water depth : d = 1.0 m ; air tunnel height : h = 1.5 m

Visualisation of the surface motions by a water surface slope imaging system

⇒ simultaneous measurements of the along- and cross-wind wave slope components

The two-component wave slope imaging system

Sideview of the slope imaging system

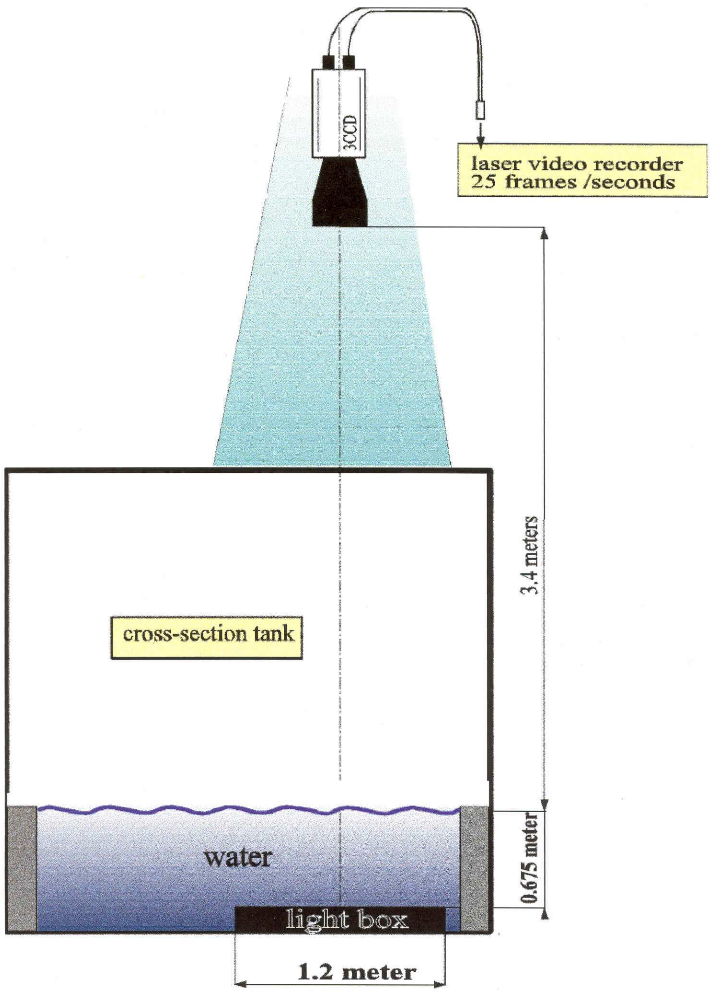

View from above of the light box

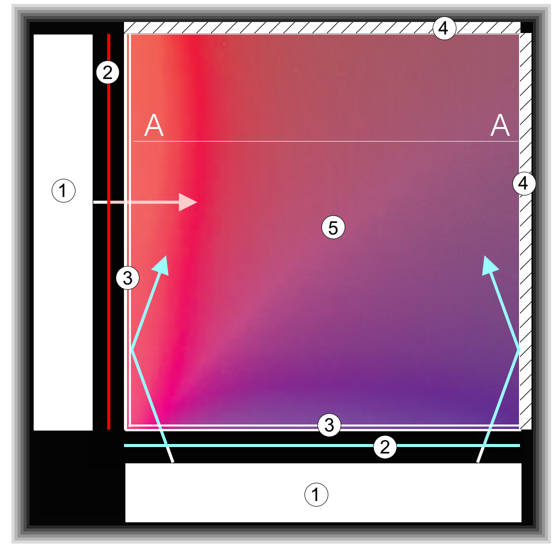

slope image recorded by the camera

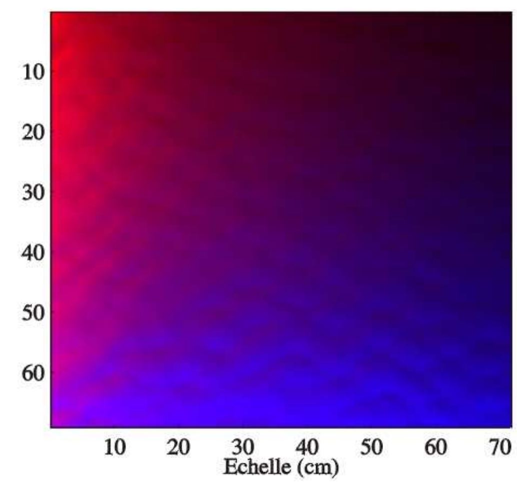

The experimental conditions

⇒ observations made for various combination of wind speed and fetch and then, of wavelength and wave steepness

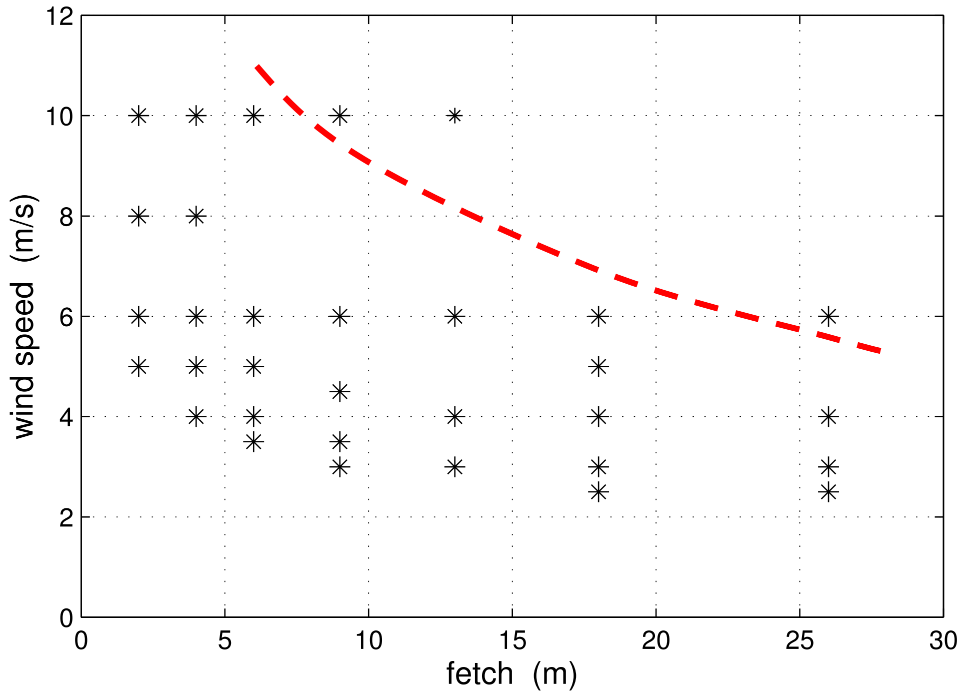

U varies from 2.5 m/s to 10 m, X from 2 to 26 m

Evolution of wavelength with fetch and wind speed

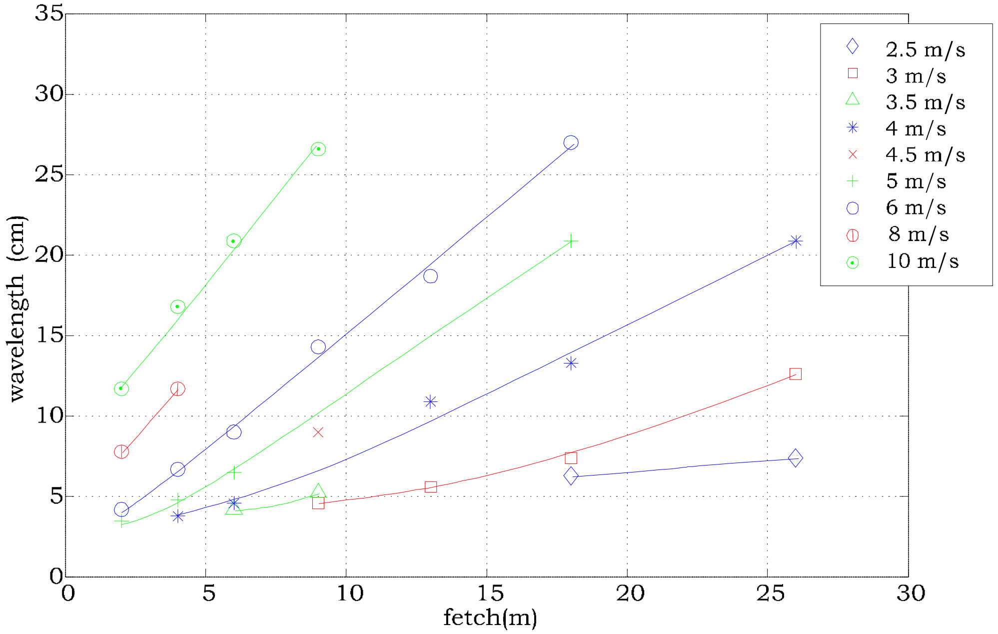

$$\eta = a \cos(\underline{\mathbf{k}}.\underline{\mathbf{x}} - \omega t),$$

η : water surface elevation

wavelength : $\lambda = 2\pi / k$

$$\eta_x = -ak_x \sin(\underline{\mathbf{k}}.\underline{\mathbf{x}} - \omega t),$$

$$\eta_y = -ak_y \sin(\underline{\mathbf{k}}.\underline{\mathbf{x}} - \omega t),$$

η_x, η_y : wave slope components

wave steepness: $\gamma = (\eta_x^2 + \eta_y^2)^{1/2}$

Evolution of wave steepness with fetch and wind speed

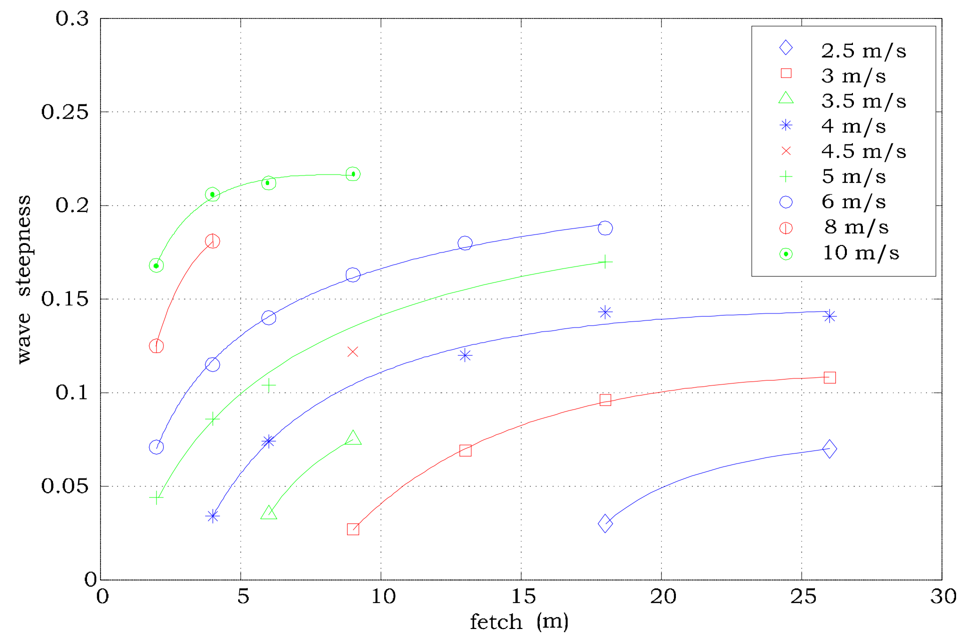

Typical time records of the water surface elevation

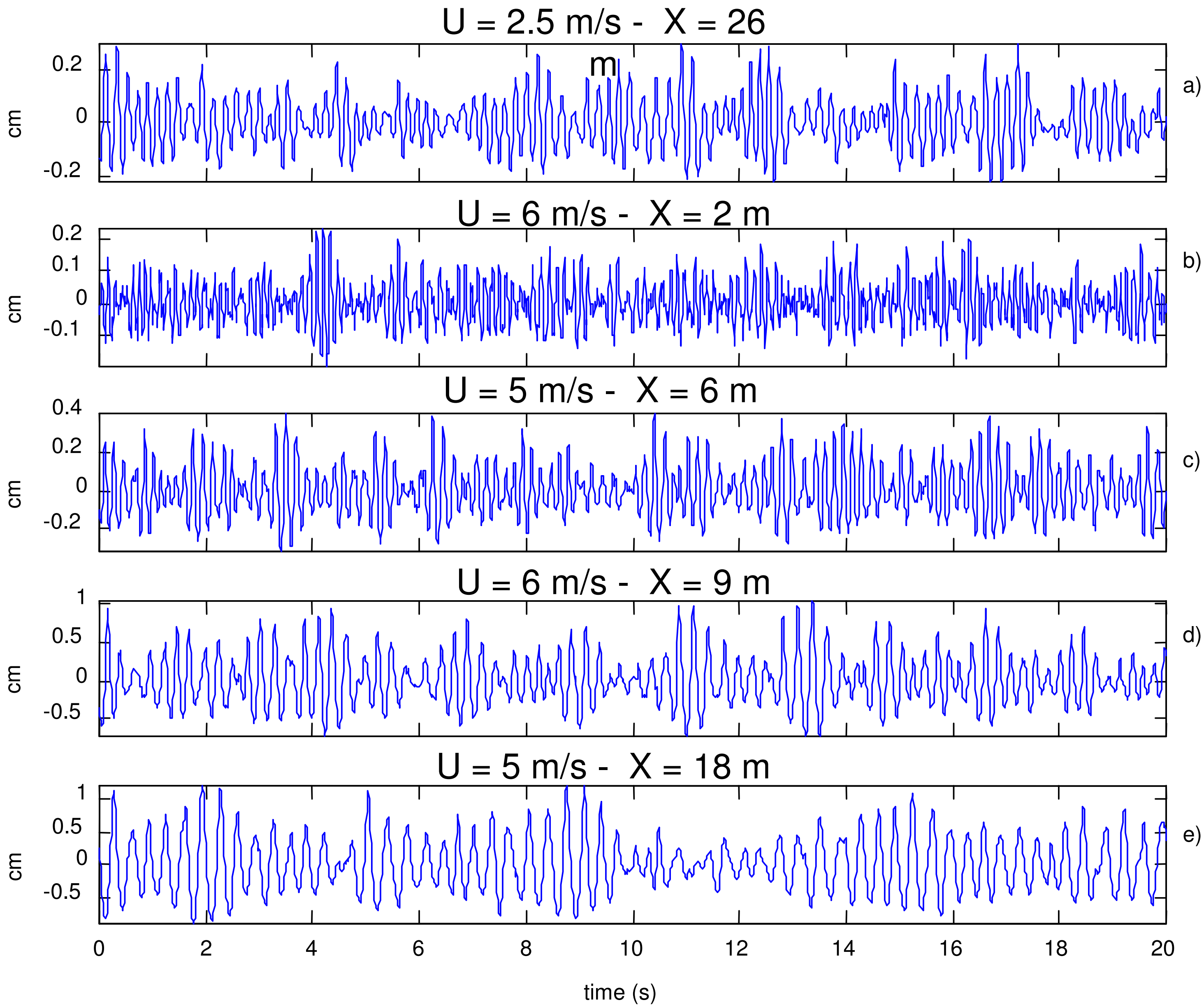

The wave amplitude varies from about 1 millimeter to few centimeters but varies in time due to the presence of wave groups whatever the wind and fetch conditions.

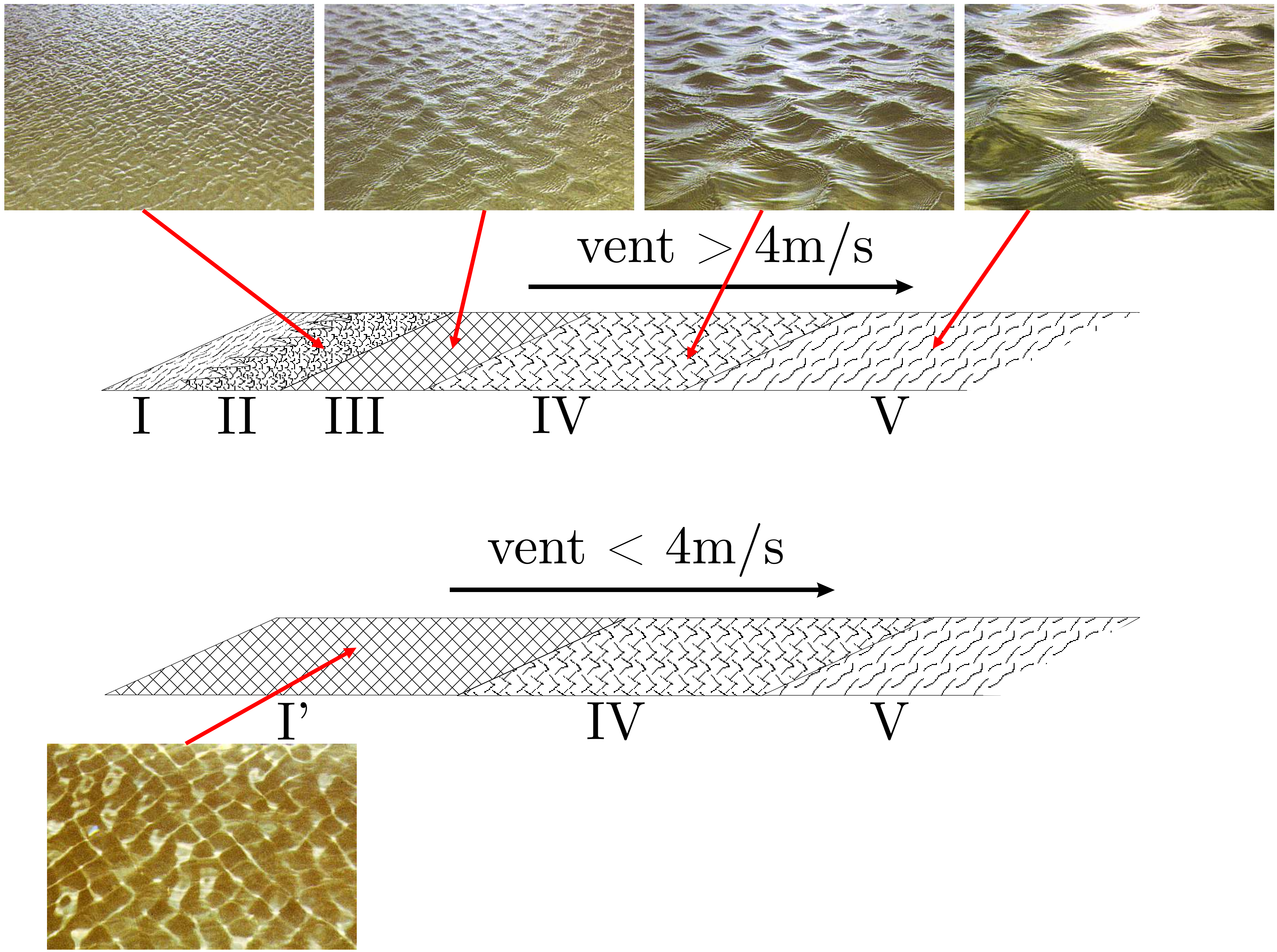
vent > 4m/s
I
II
III
IV
V
vent < 4m/s
I'
IV
V

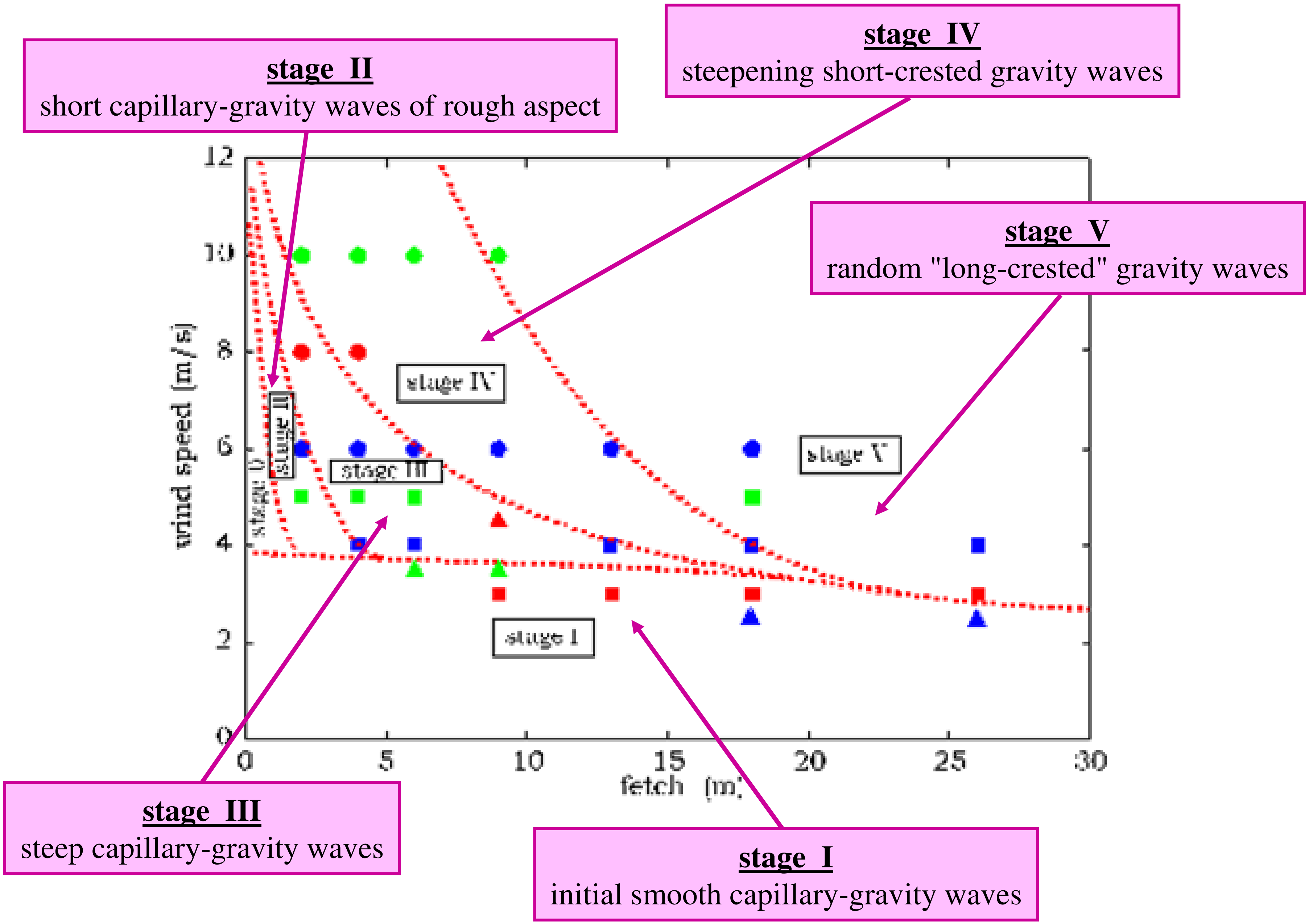
stage II
short capillary-gravity waves of rough aspect
stage IV
steepening short-crested gravity waves
stage V
random "long-crested" gravity waves
stage III
steep capillary-gravity waves
stage I
initial smooth capillary-gravity waves
wind speed (m/s)
fetch (m)
stage IV
stage III
stage V
stage I
0
2
4
6
8
10
12
0
5
10
15
20
25
30

U = 6 m/s – X = 2 m

Stage II

Sideview of the wave field

U

alongwind slope

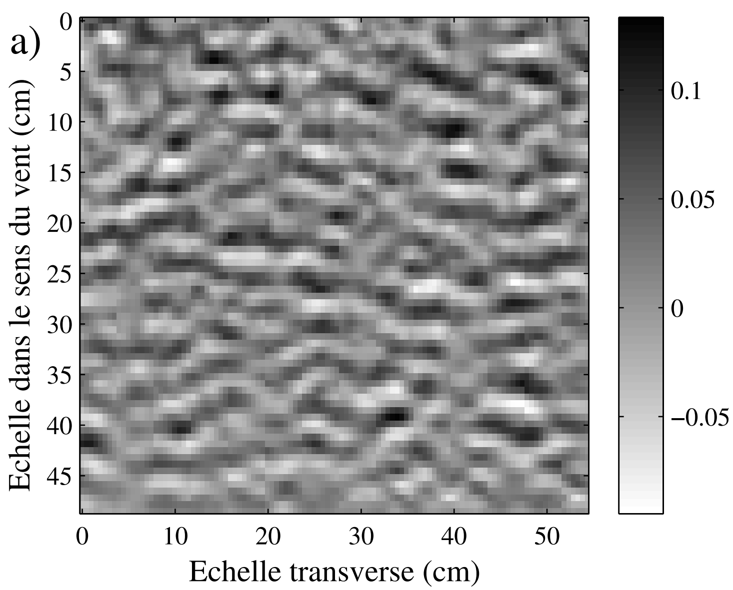

crosswind slope

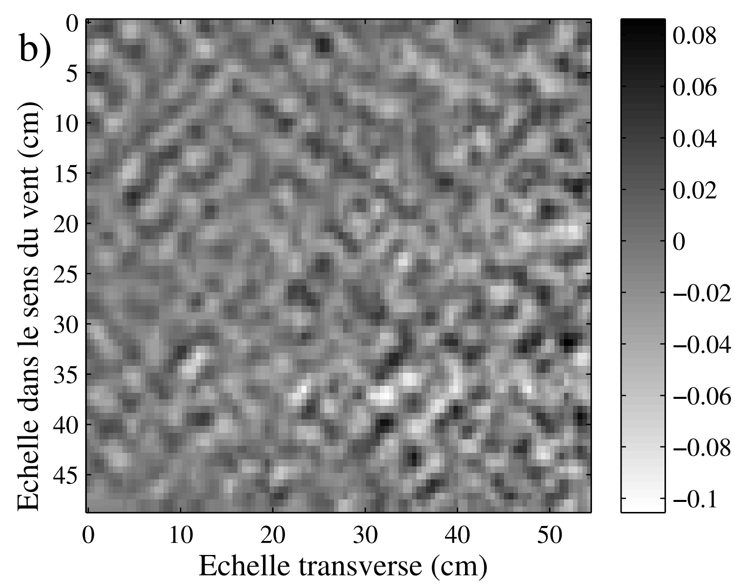

U = 6 m/s – X = 2 m

Stage II

Two-dimensional wave slope spectrum S(k,θ)

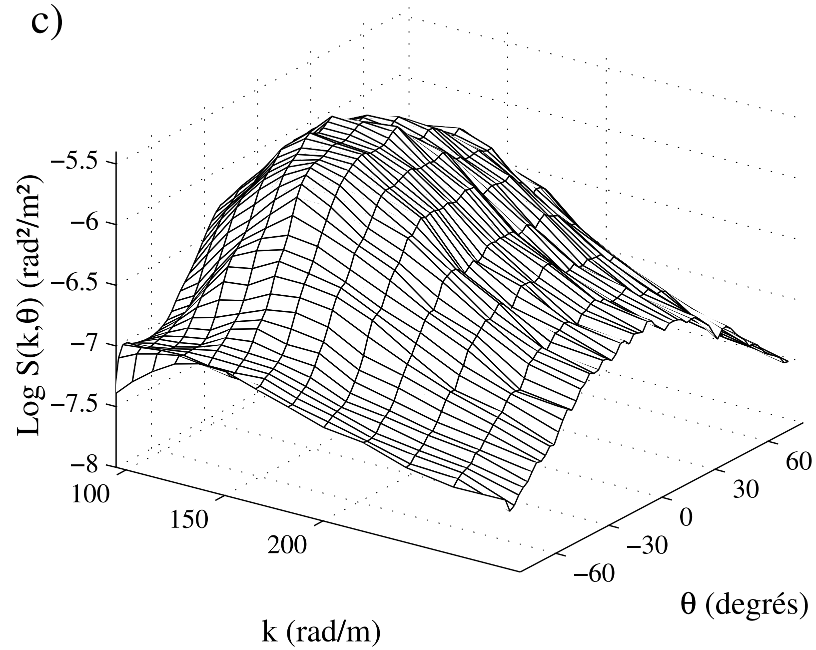

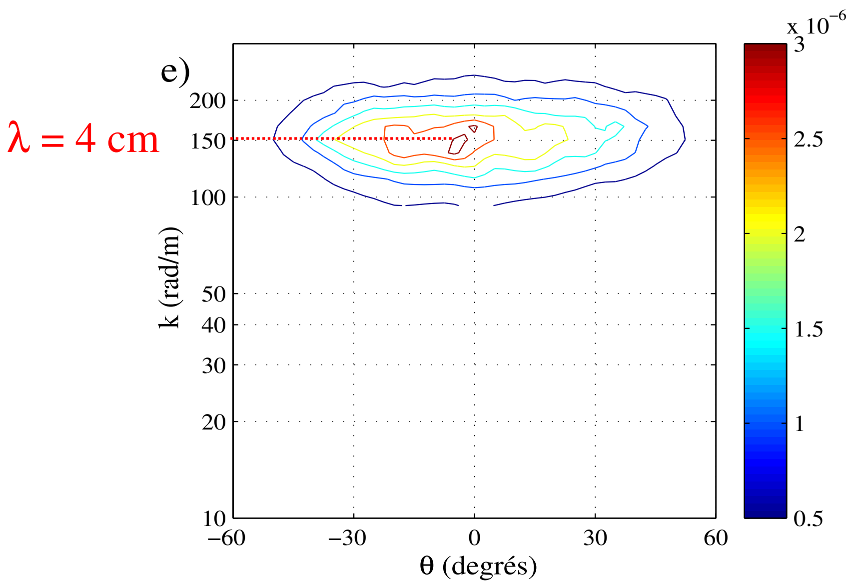

Contour lines

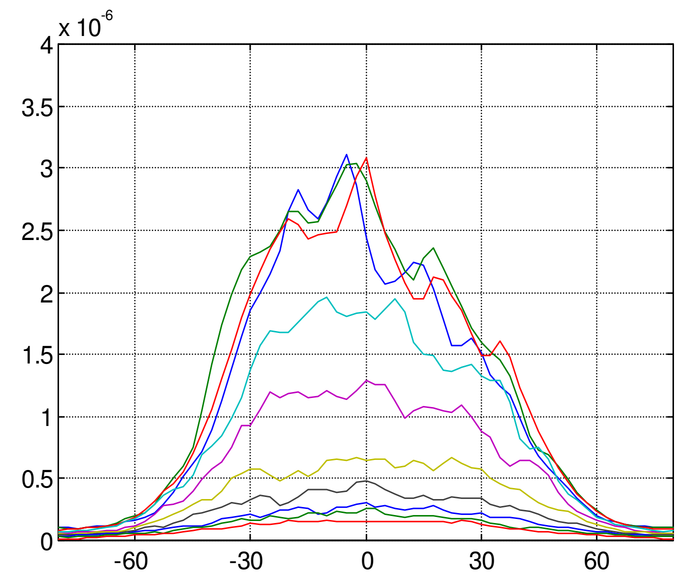

Constant-k plan sections ($k > k_{peak}$)

U = 5 m/s – X = 6 m

<u>Stage III</u>

The wave field is composed of two oblique waves, exhibiting characteristic rhombic patterns

<u>Side view of the wave field</u>

U

<u>alongwind slope</u>

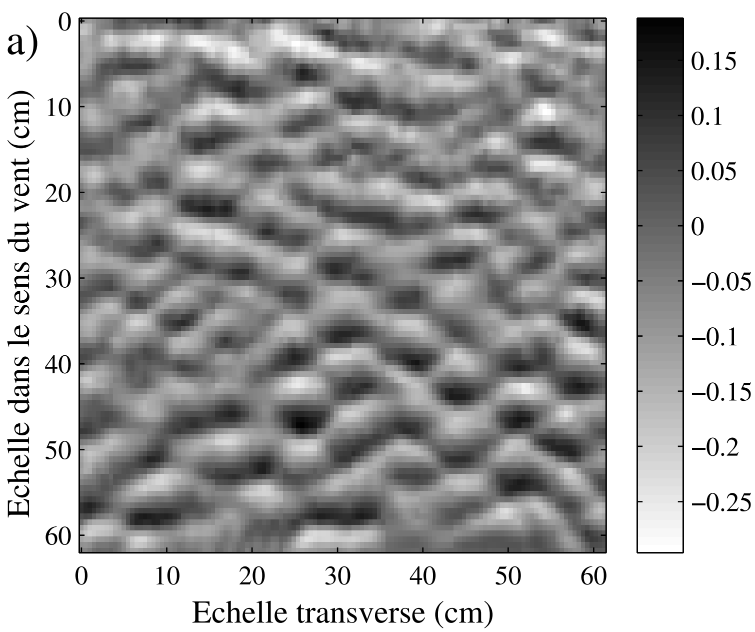

<u>crosswind slope</u>

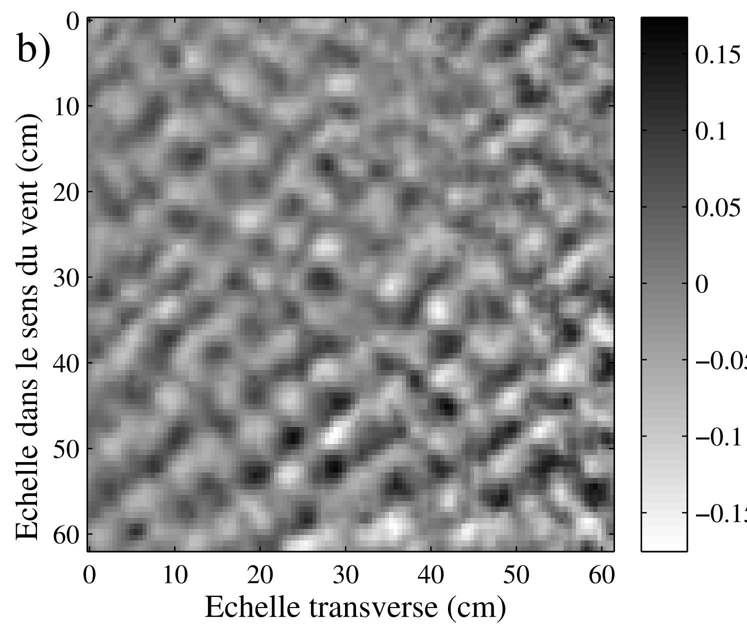

U = 5 m/s – X = 6 m

Stage III

Two-dimensional wave slope spectrum S(k,θ)

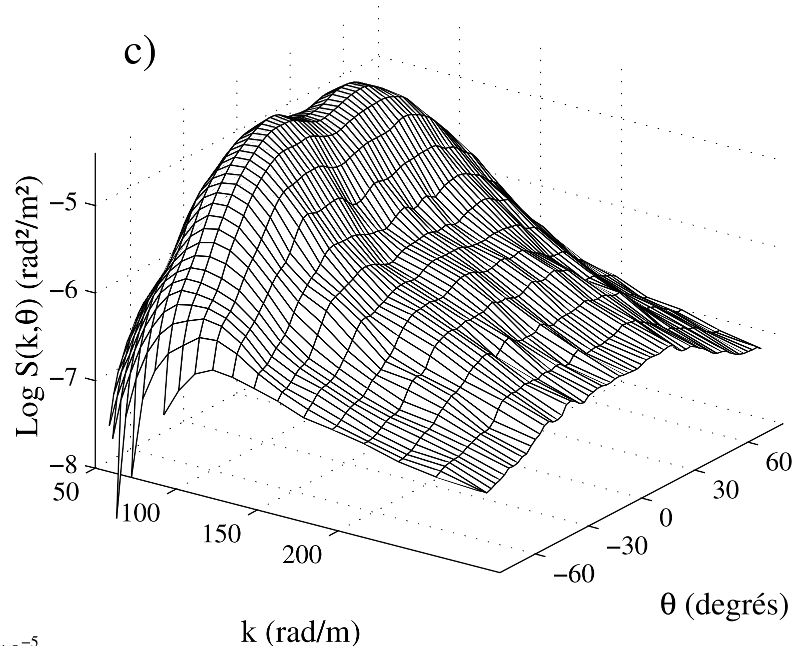

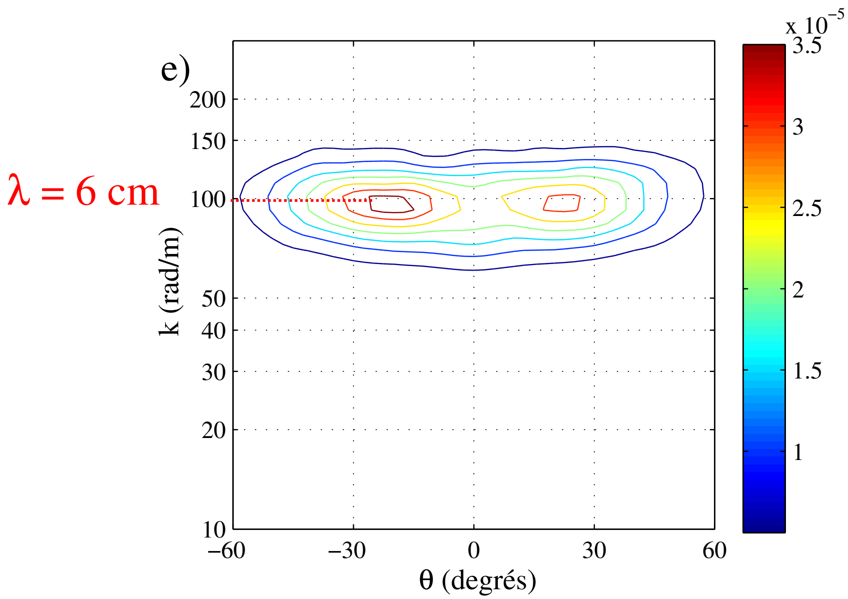

Contour lines

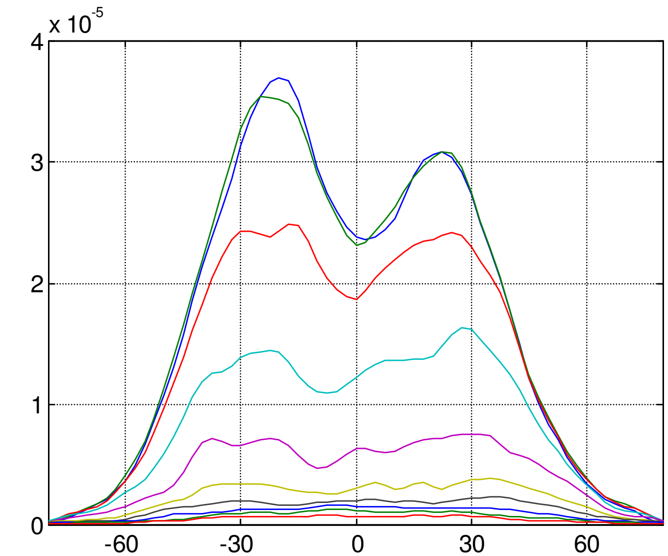

Constant-k plan sections ($k > k_{peak}$)

U = 6 m/s – X = 9 m

Stage IV

The wave field is composed of characteristic short-crested waves, but distributed more randomly

Sideview of the wave field

U

alongwind slope

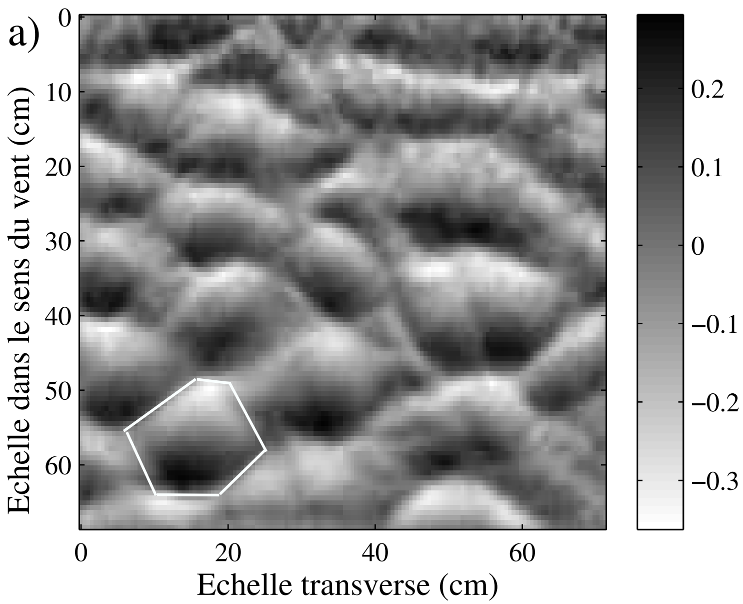

crosswind slope

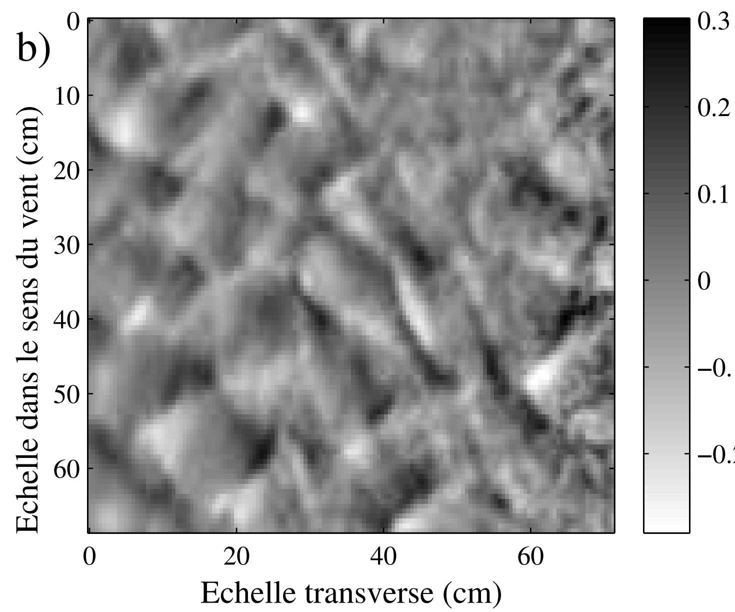

U = 6 m/s – X = 9 m

Stage IV

Two-dimensional wave slope spectrum S(k,θ)

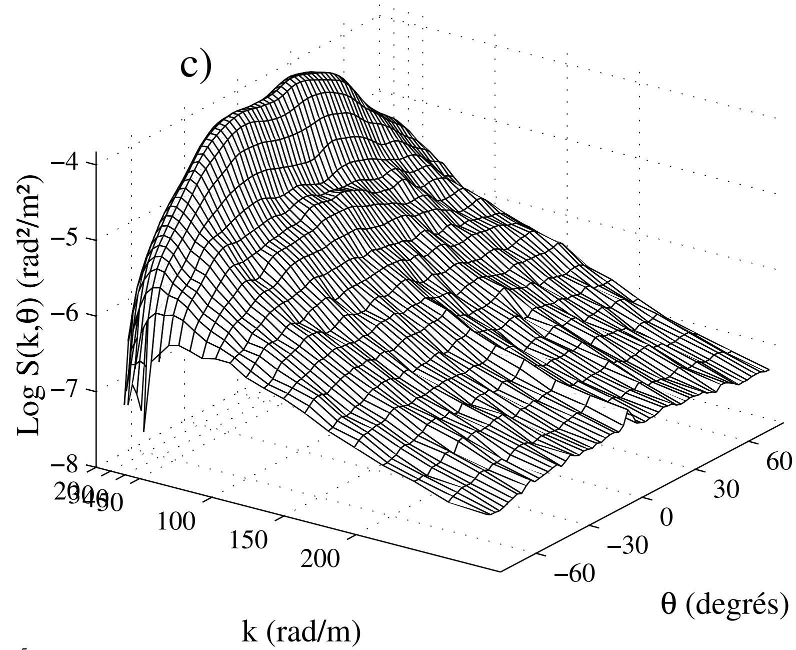

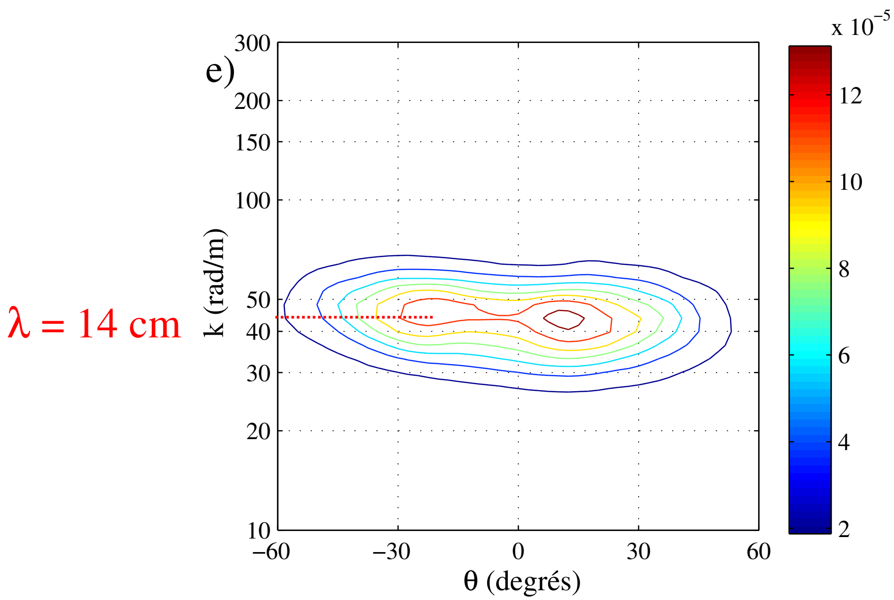

Contour lines

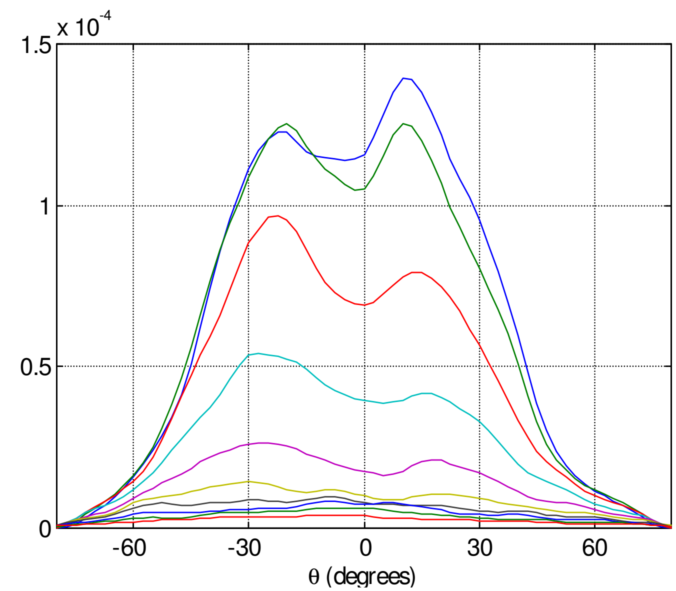

Constant-k plan sections ($k > k_{peak}$)

U = 5 m/s – X = 18 m

Stage V

The wave field is composed of short gravity waves with intermittent long or crescent-shaped crests, exhibiting random 3D patterns

Sideview of the wave field

U

alongwind slope

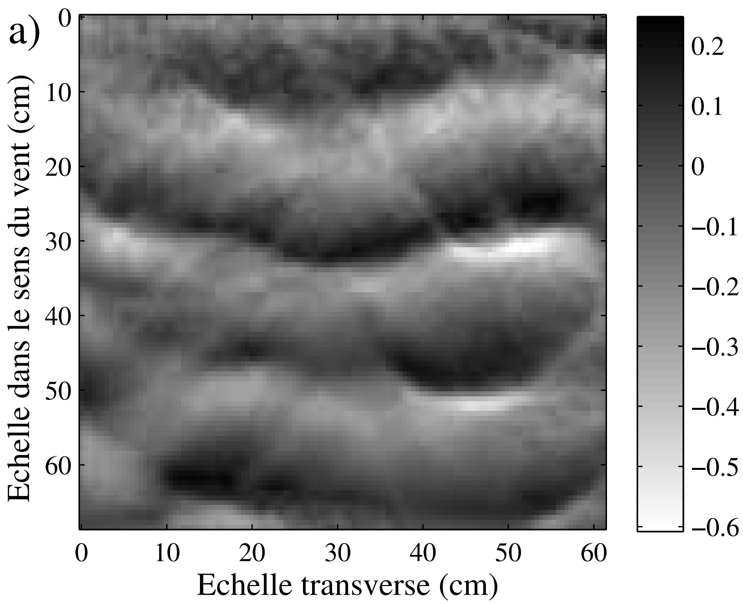

crosswind slope

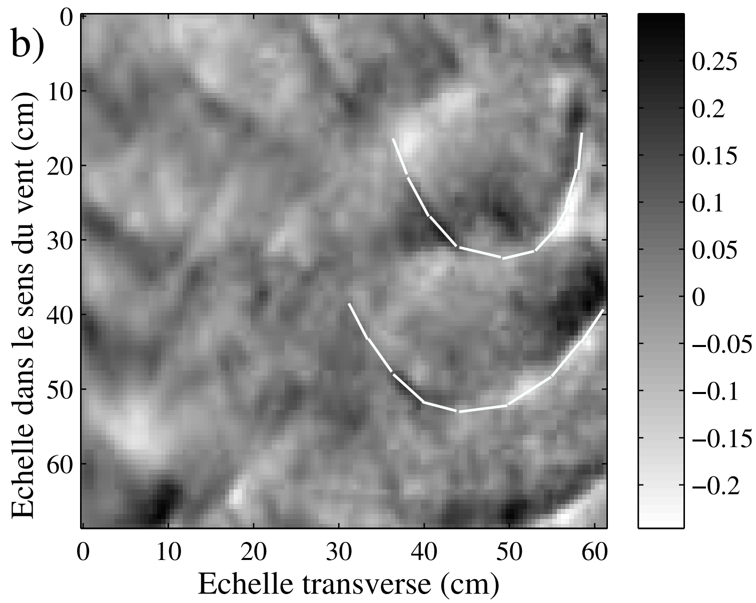

U = 5 m/s – X = 18 m

Stage V

Two-dimensional wave slope spectrum S(k,θ)

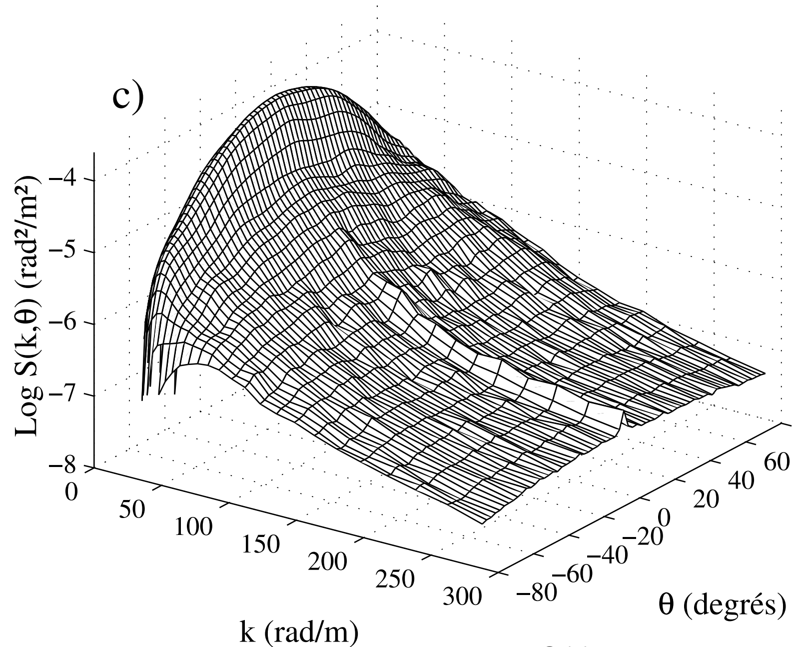

λ = 20 cm

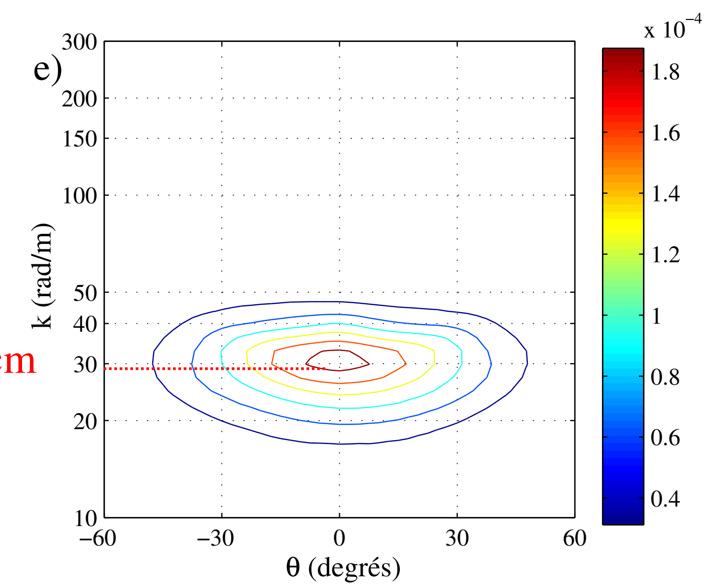

Contour lines

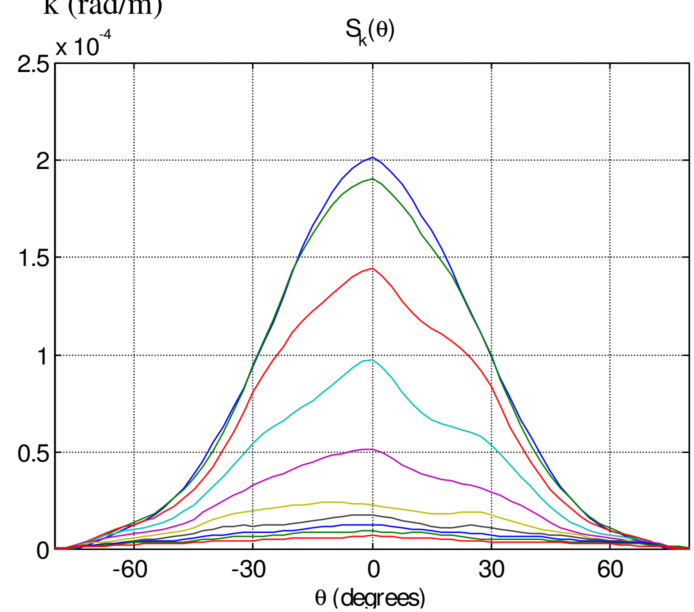

Constant-k plan sections ($k > k_{peak}$)

U = 2.5 m/s - X = 26 m

Stage I

The wave field is composed of two oblique waves of very small amplitude varying both in space and time

Sideview of the wave field

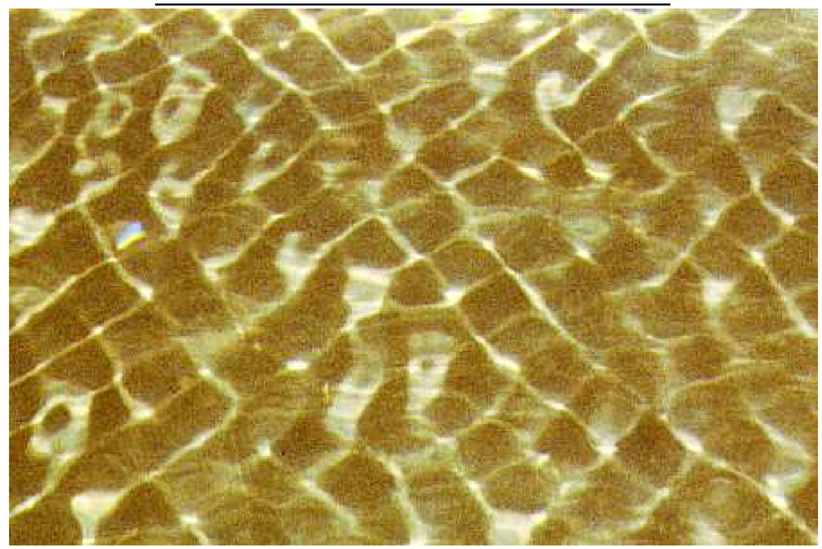

U

alongwind slope

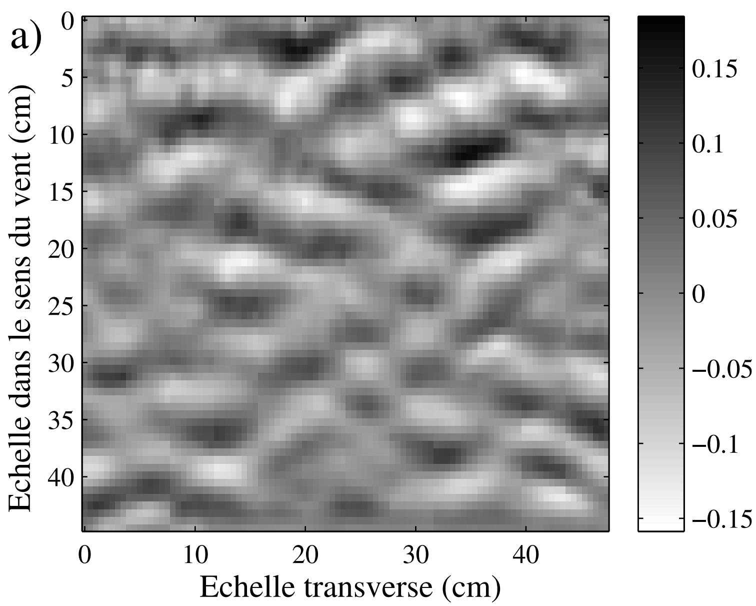

crosswind slope

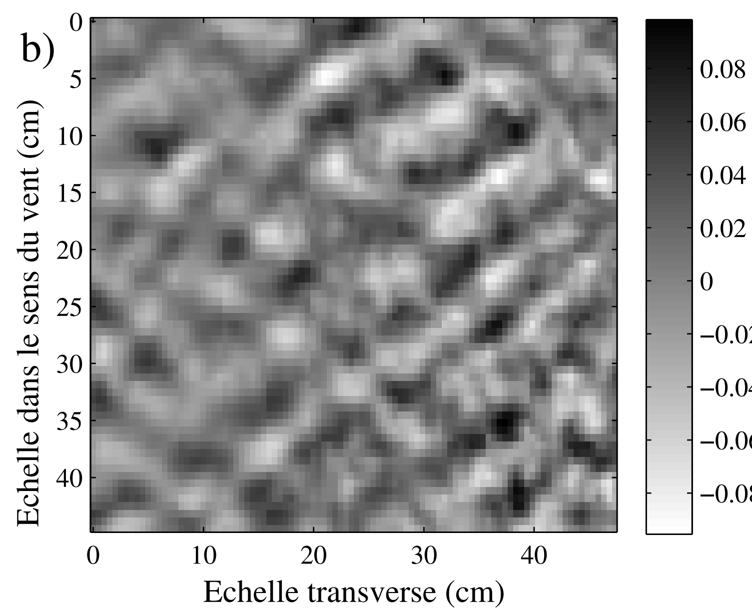

U = 2.5 m/s – X = 26 m

Stage I

Two-dimensional wave slope spectrum S(k,θ)

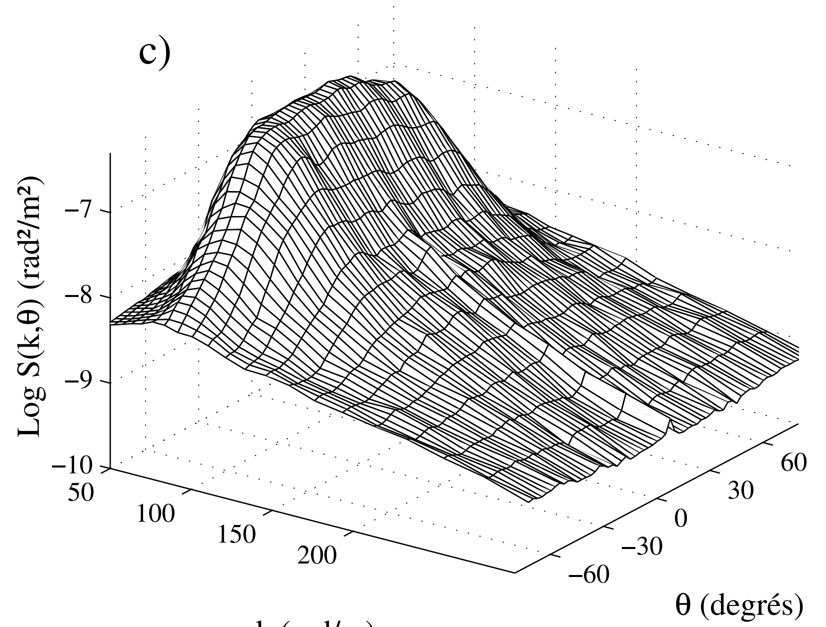

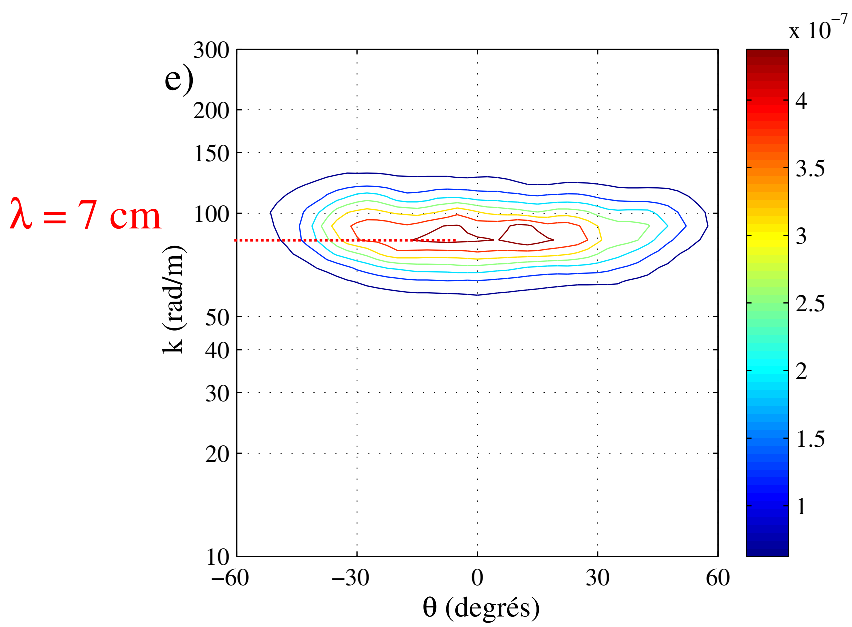

Contour lines

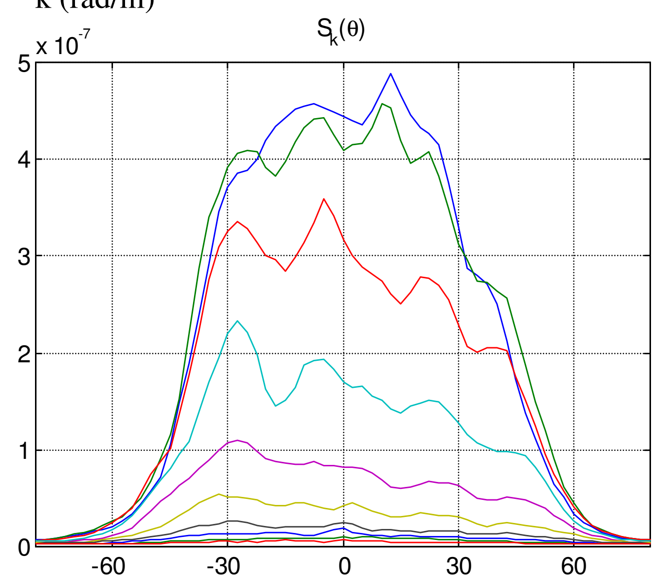

Constant-k plan sections ($k > k_{peak}$)

Pattern Analysis

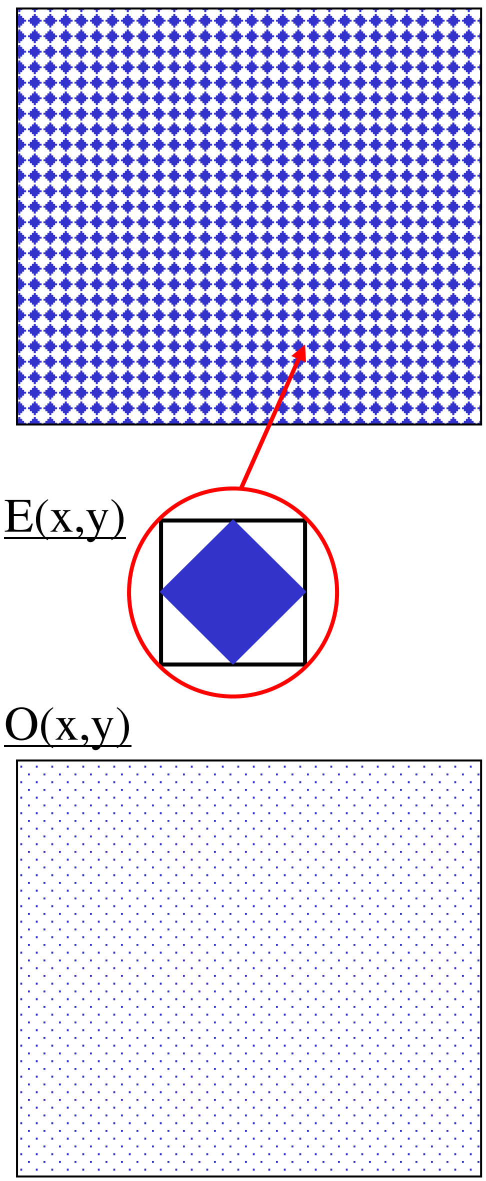

⇒ Method used to analyze local patterns of particular shape organized regularly at a surface and to determine the shape (the "elementary pattern") and the location in space of the patterns (the "structural image").

The elementary pattern E(x,y)

1. Use of an autocorrelation method to estimate the characteristic scales of the elementary pattern: minima of the autocorrelation function in the alongwind and crosswind directions;
2. Estimation of the shape of the elementary pattern E(x, y) by averaging small rectangular images centered on characteristic features of the water surface elevation image $\eta(x,y)$.

The structural image O(x,y)

1. Estimation of the cross-correlation function C(x, y) between the elementary pattern E(x,y) and the surface image $\eta(x,y)$;
2. Determination of the location of the elementary patterns O(x,y) as the position in space of the maxima of the cross-correlation function:

$$O(x, y) = C(x, y) \quad \text{if } C_{x,y}(x,y) = 0;$$
$$O(x, y) = 0 \quad \text{elsewhese.}$$

Water surface elevation

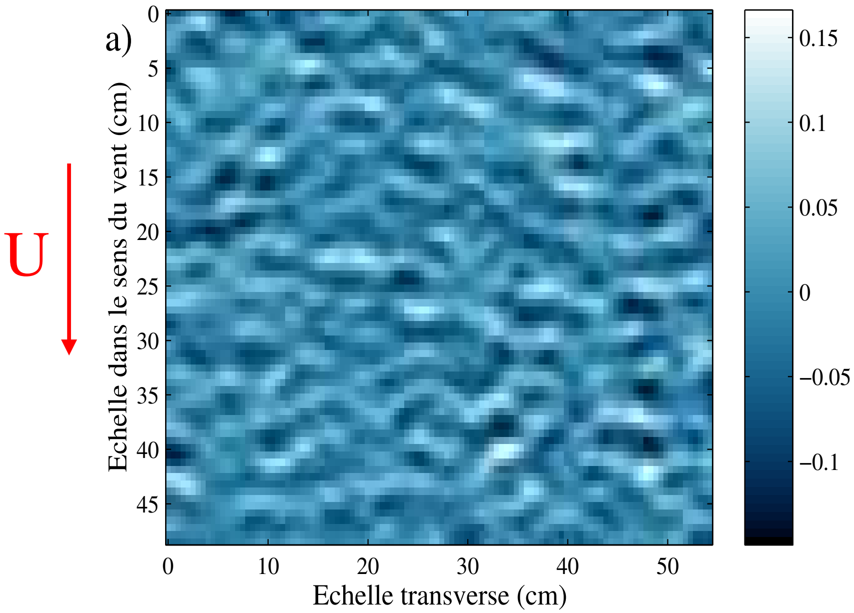

U = 6 m/s – X = 2 m

Stage II

Mean coherency: 0.49

Elementary pattern

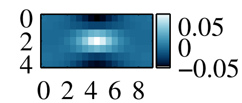

Surface/pattern cross-correlation

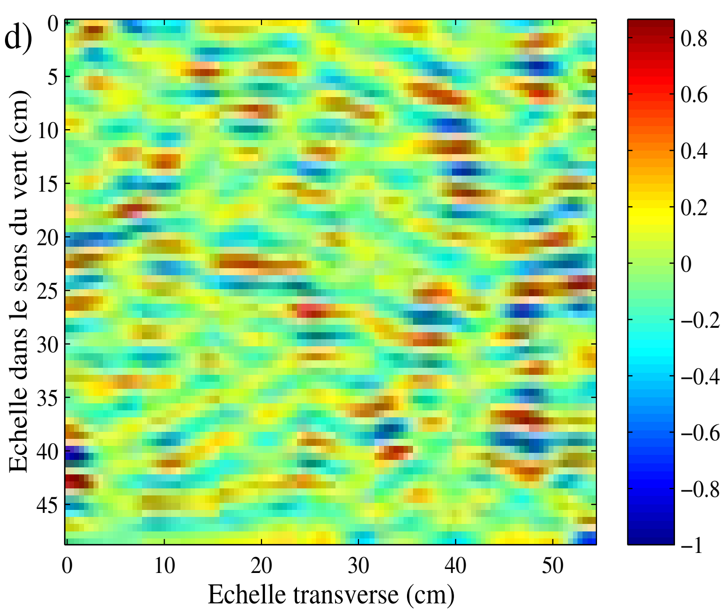

Structural image

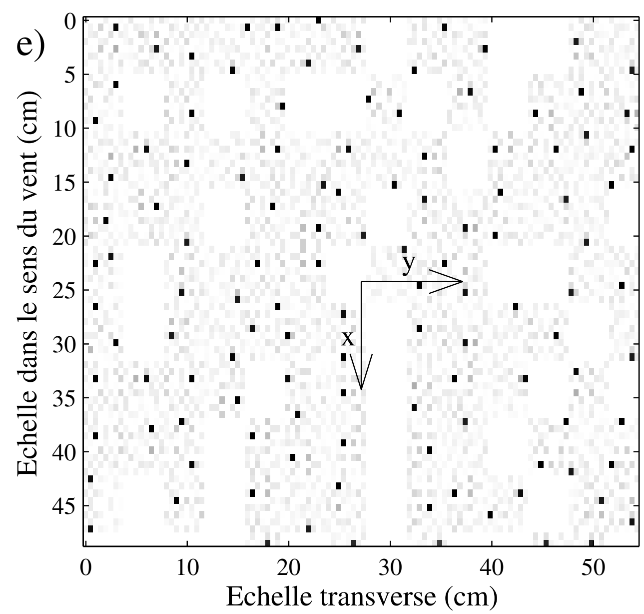

U = 6 m/s – X = 2 m

Stage II

Two-dimensional spectrum of the structural images

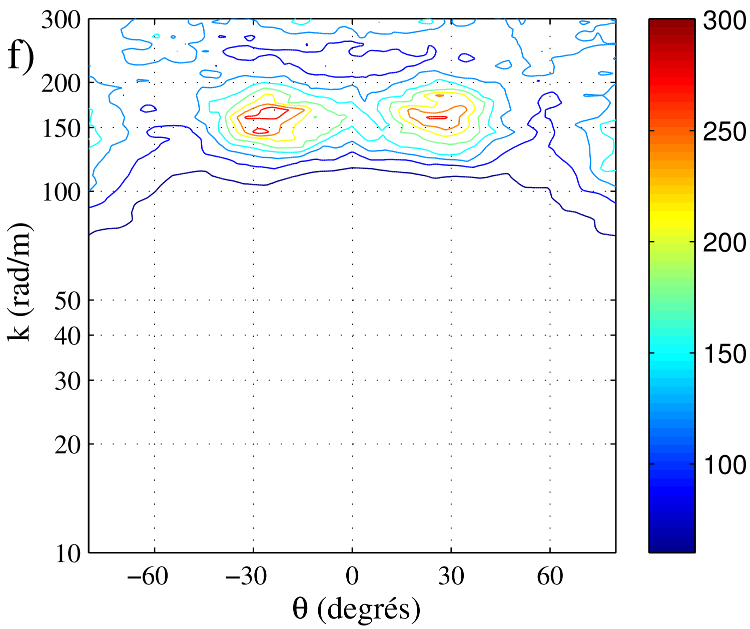

Contour lines

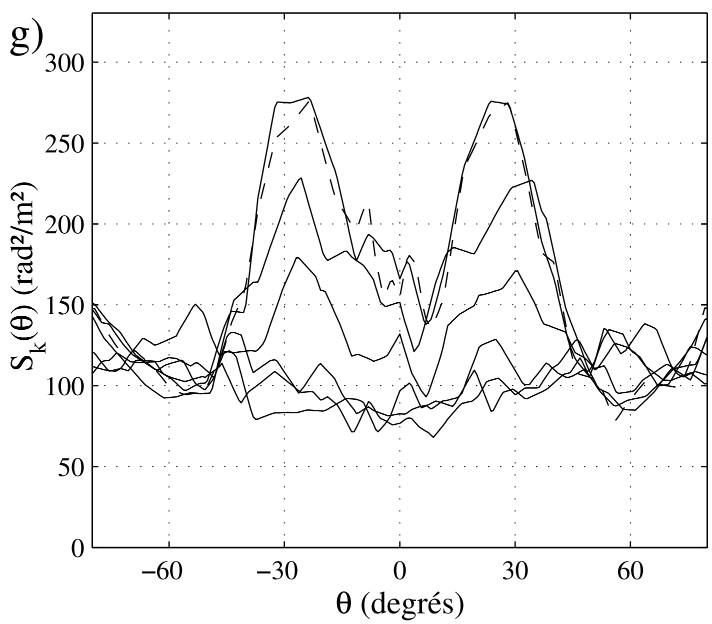

Constant-k plan sections ($k > k_{peak}$)

half peak width: 40°

Water surface elevation

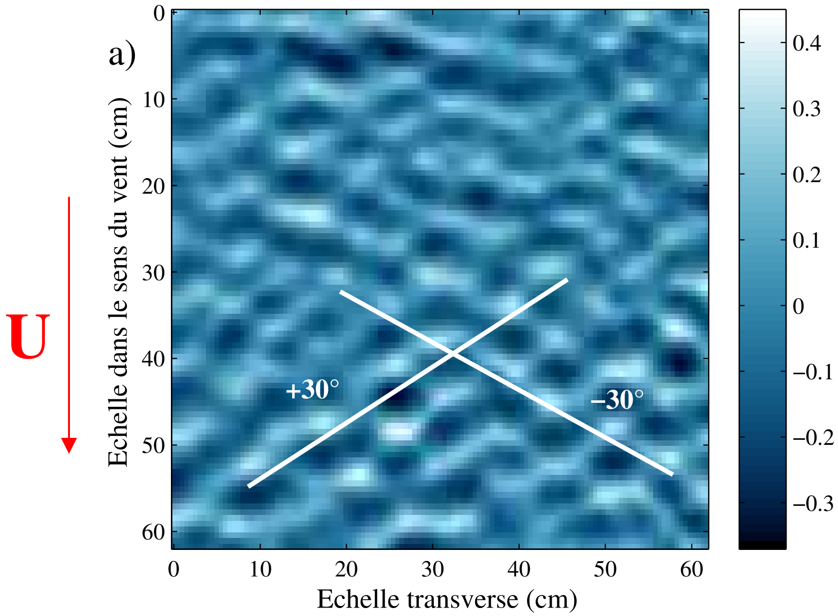

U = 5 m/s – X = 6 m

Stage III

Mean coherency: 0.60

Elementary pattern

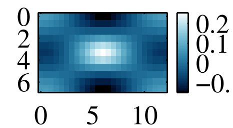

Surface/pattern cross-correlation

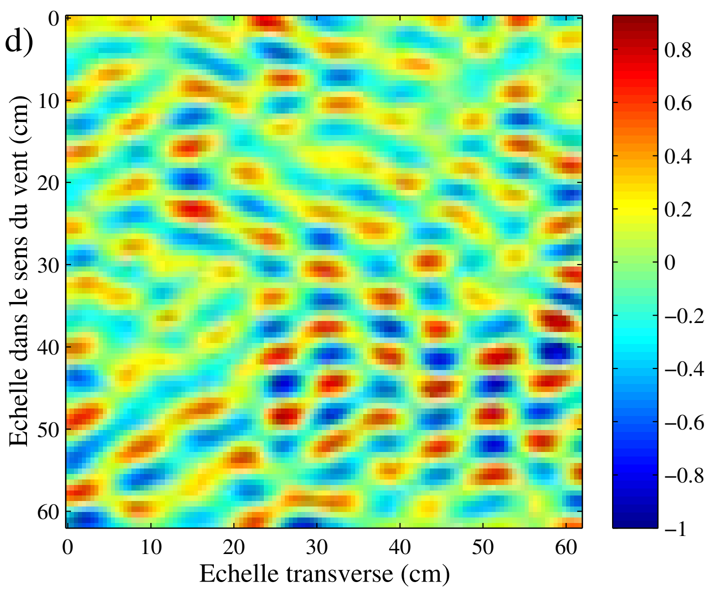

Structural image

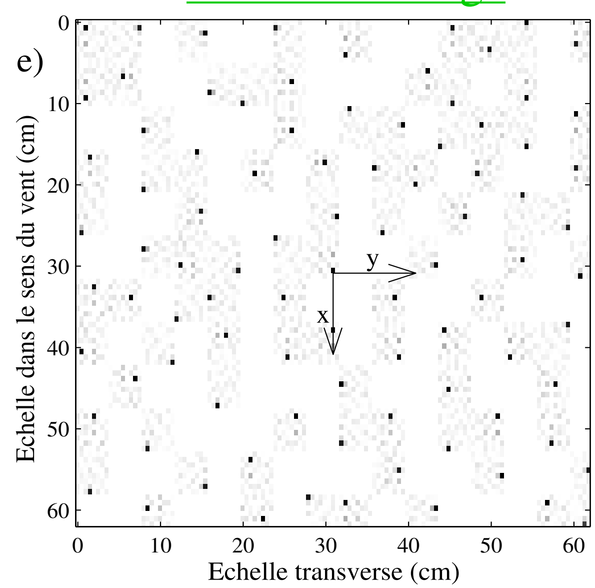

U = 5 m/s – X = 6 m

Stage III

Two-dimensional spectrum of the structural images

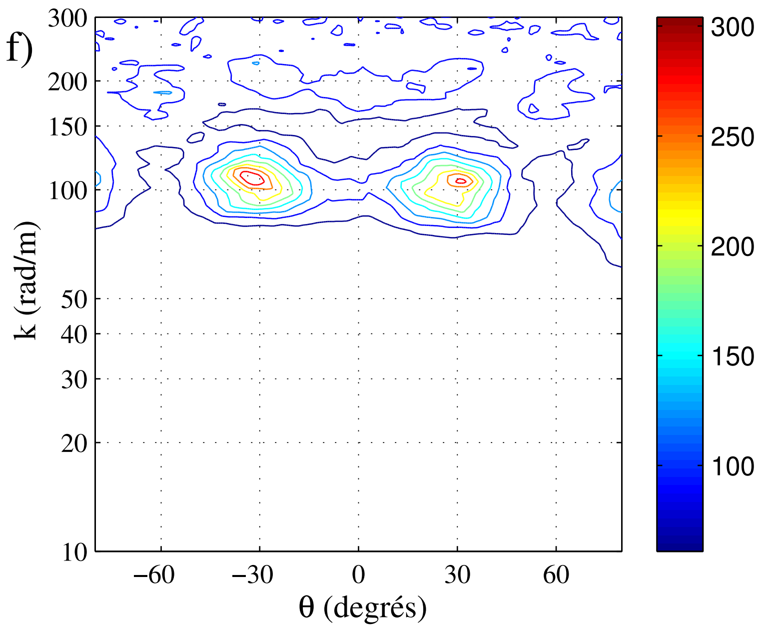

Contour lines

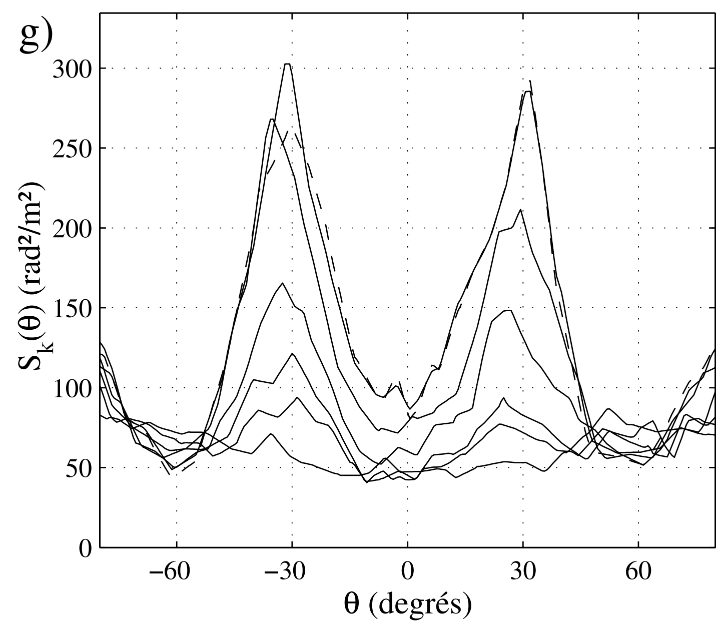

Constant-k plan sections ($k > k_{peak}$)

half peak width: 24°

Water surface elevation

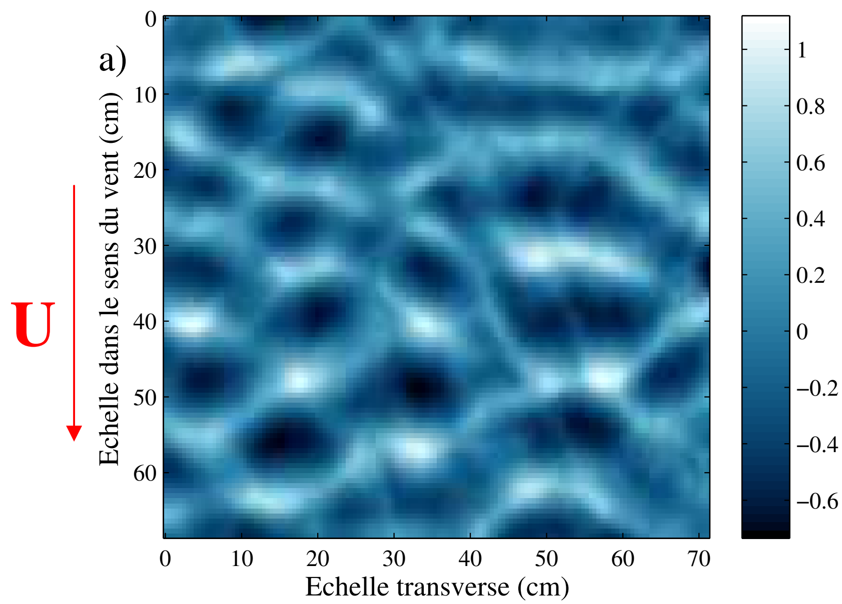

U = 6 m/s – X = 9 m

Stage IV

Mean coherency: 0.57

Elementary pattern

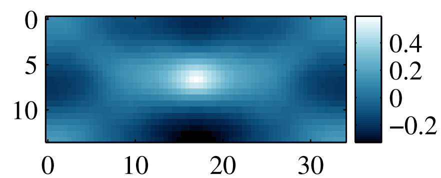

Surface/pattern cross-correlation

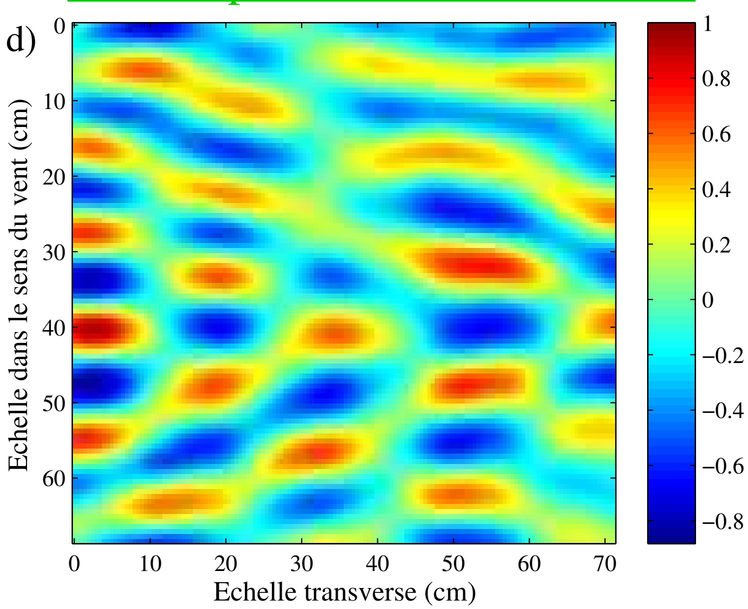

Structural image

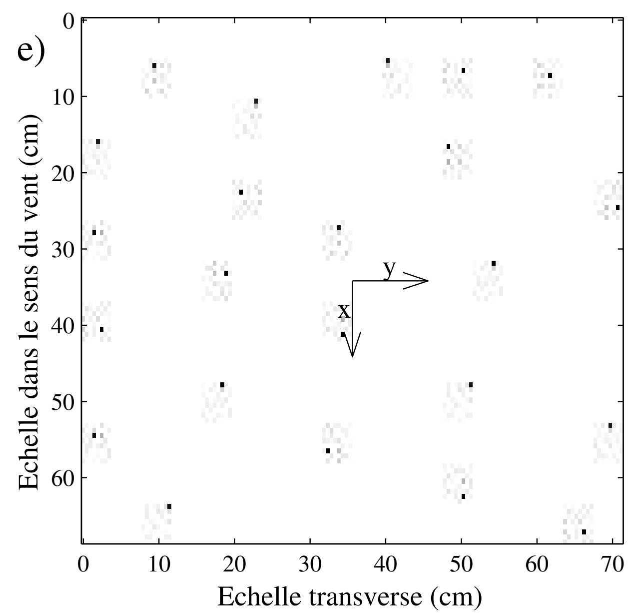

U = 6 m/s – X = 9 m

Stage IV

Two-dimensional spectrum of the structural images

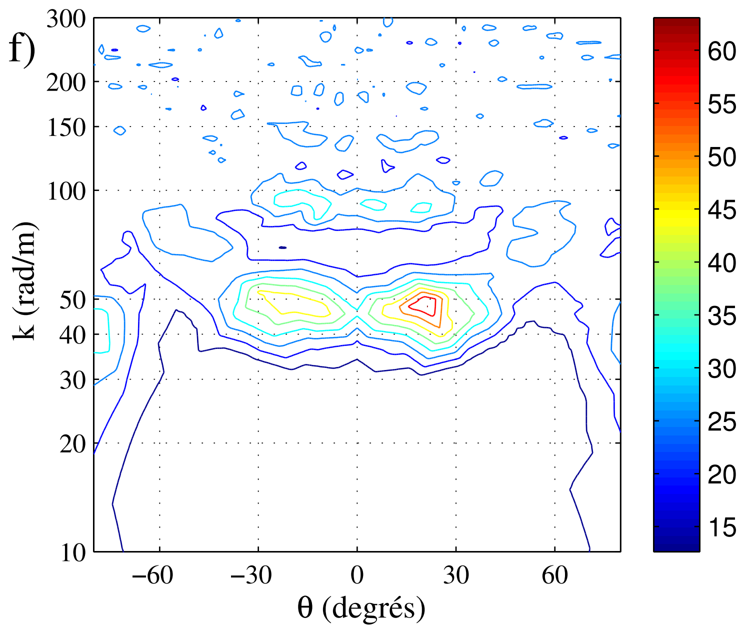

Contour lines

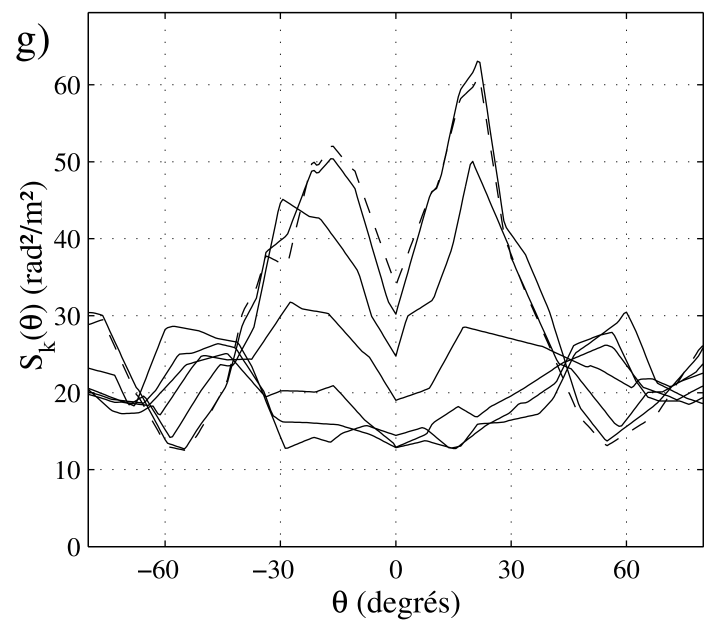

Constant-k plan sections ($k > k_{peak}$)

half peak width: 40°

U = 5 m/s – X = 18 m

Stage V

Mean coherency: 0.49

Water surface elevation

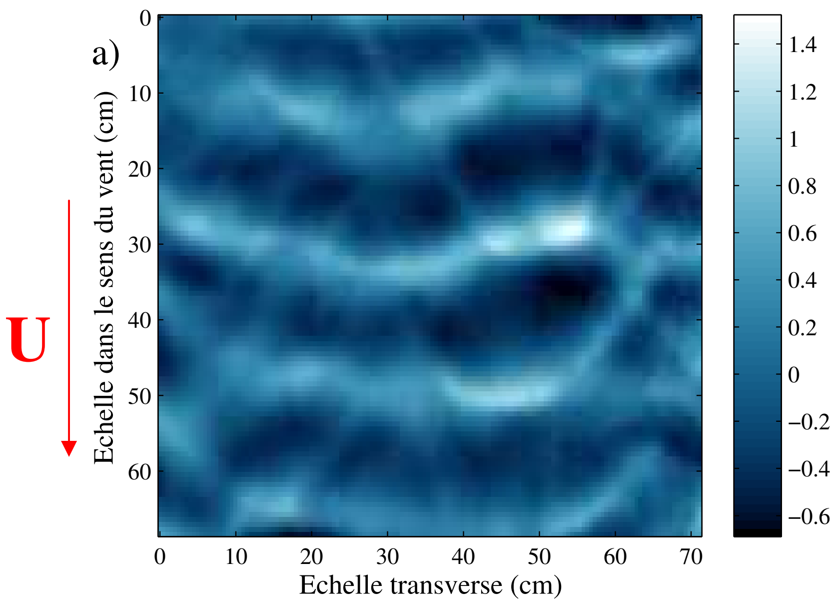

Elementary pattern

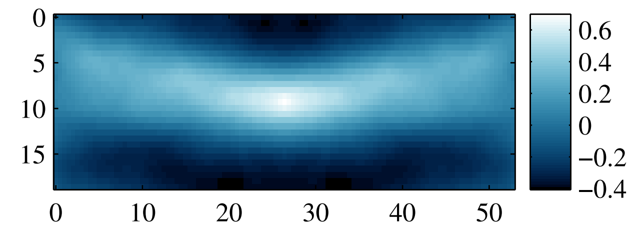

Surface/pattern cross-correlation

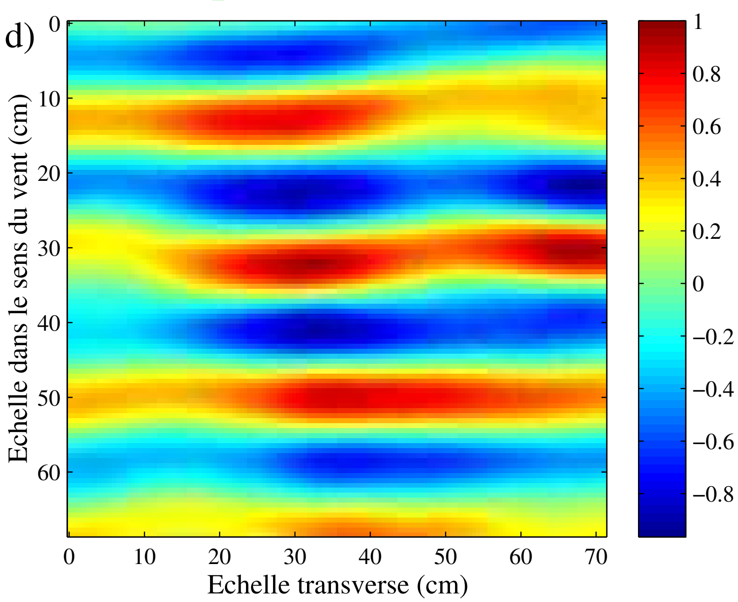

Structural image

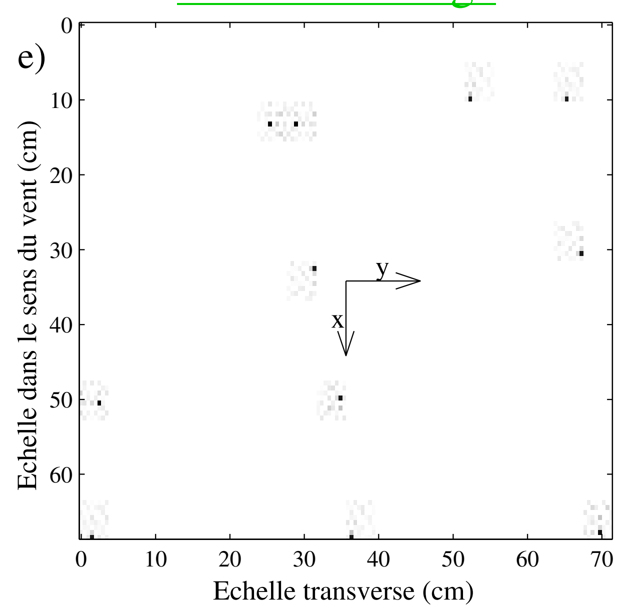

U = 5 m/s – X = 18 m

Stage V

Two-dimensional spectrum of the structural images

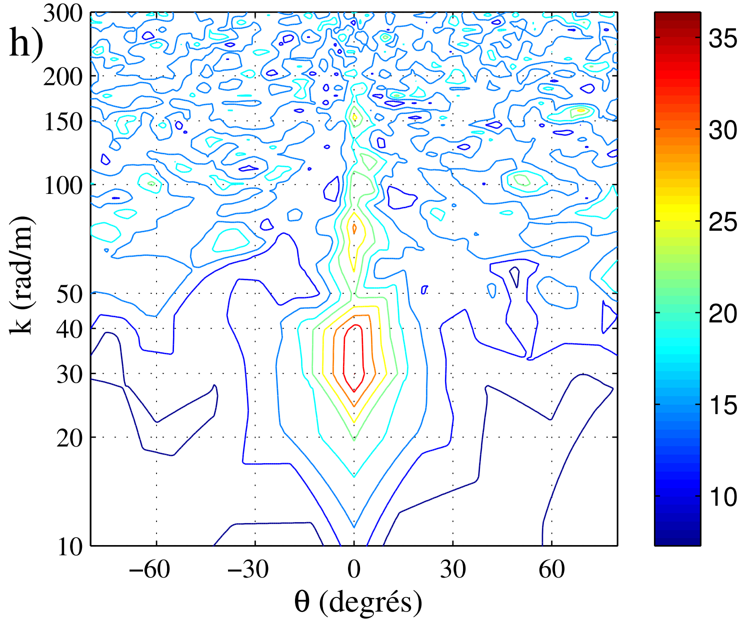

Contour lines

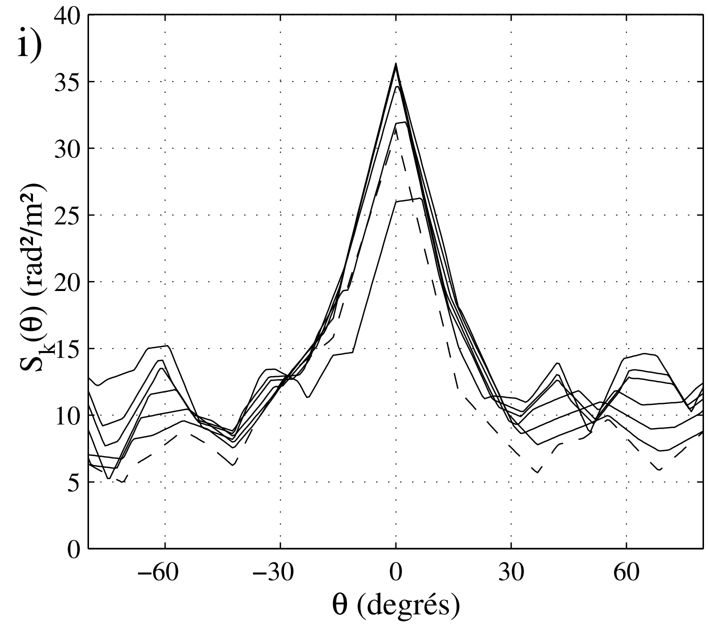

Constant-k plan sections ($k > k_{peak}$)

half peak width: 30°

Water surface elevation

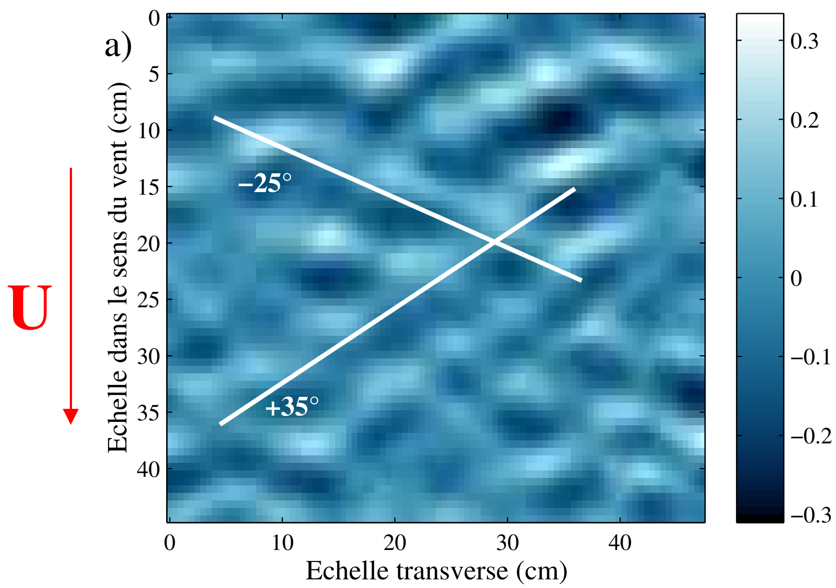

U = 2.5 m/s – X = 26 m

Stage 1’

Mean coherency: 0.58

Elementary pattern

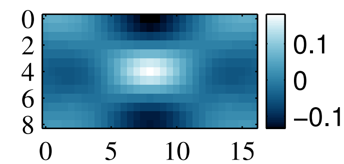

Surface/pattern cross-correlation

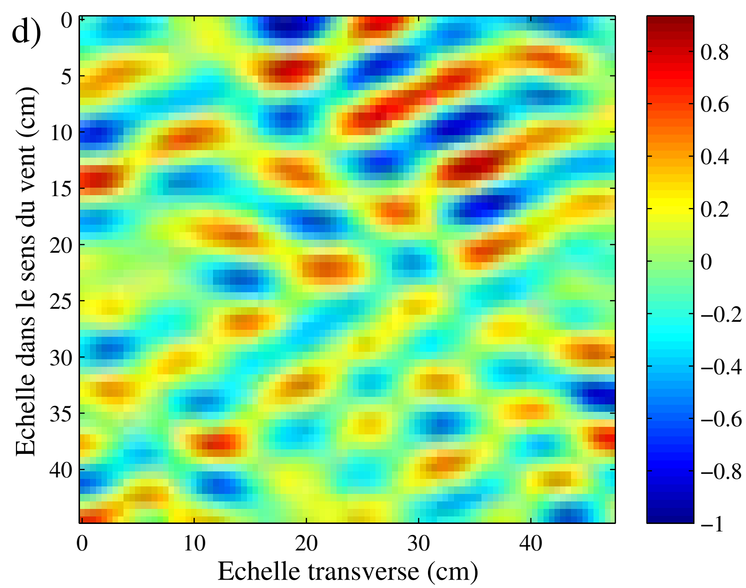

Structural image

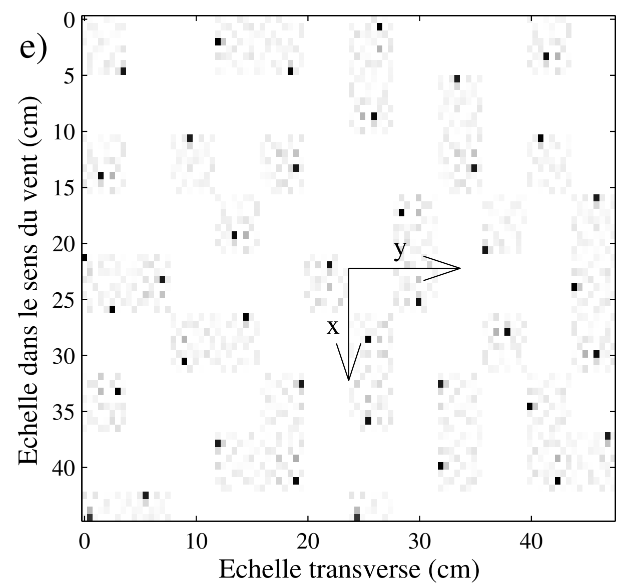

U = 2.5 m/s – X = 26 m

Stage I'

Two-dimensional spectrum of the structural images

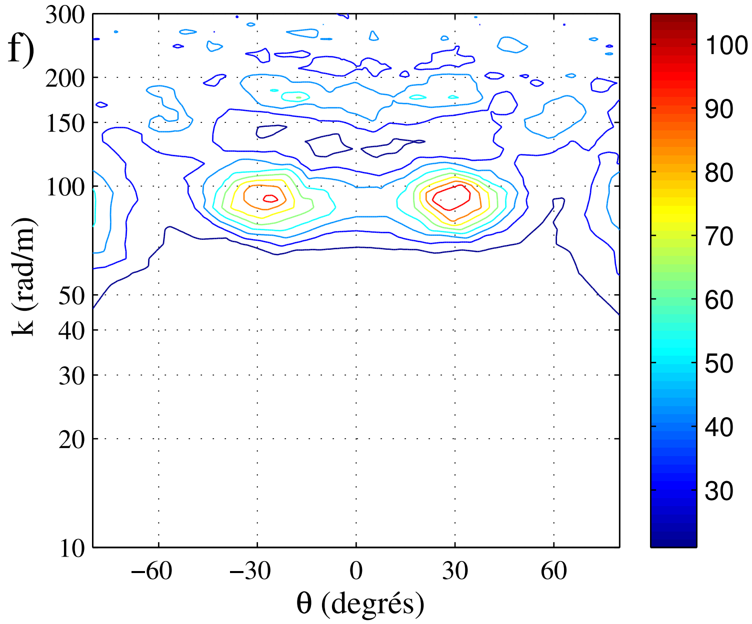

Contour lines

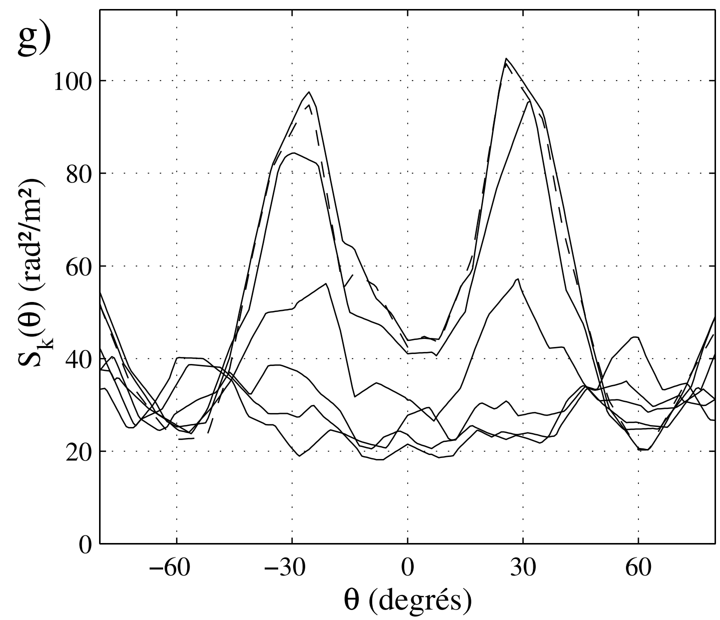

Constant-k plan sections (k > kpeak)

half peak width: 34°

Mean coherency of the pattern structure

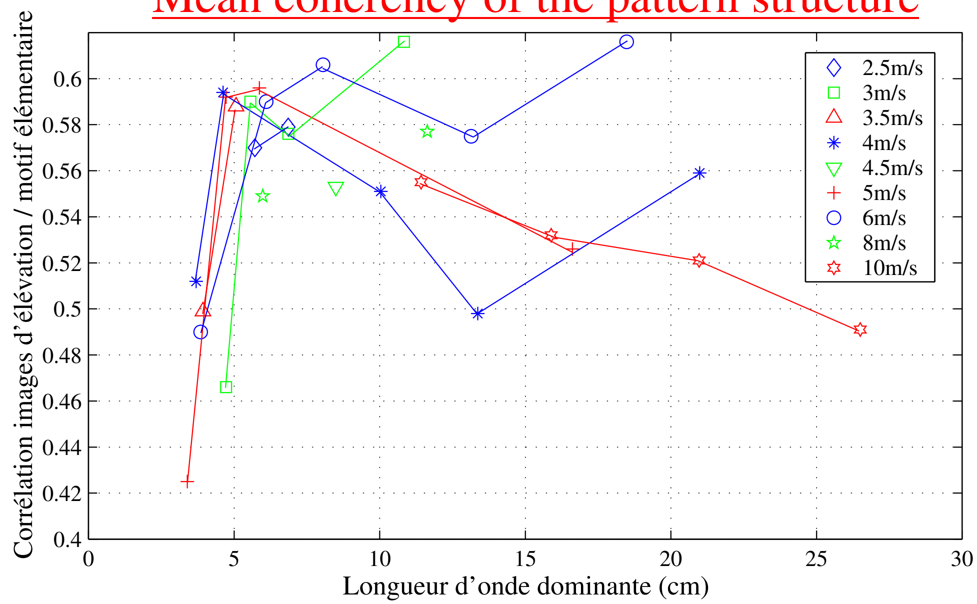

Mean direction of the pattern structure

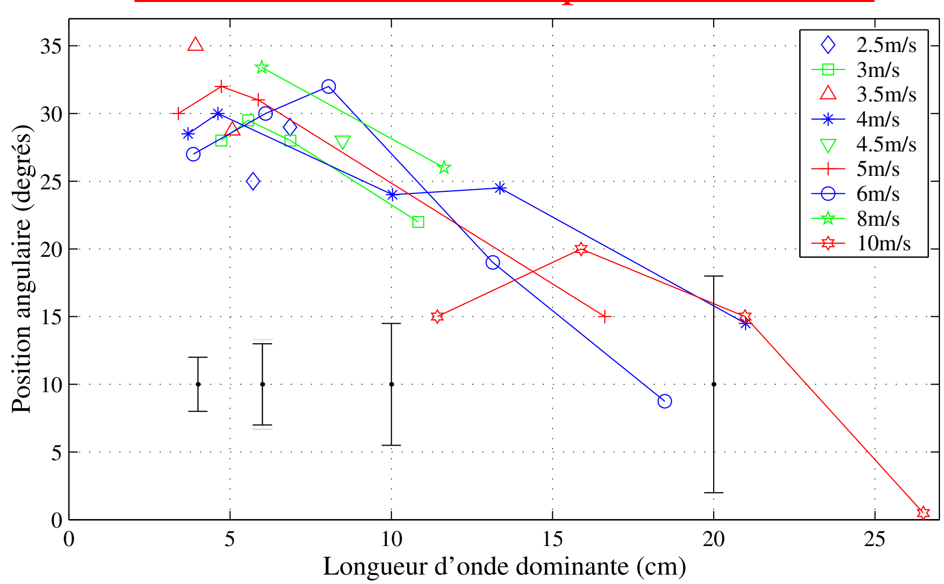

stage III

steep capillary-gravity waves

$4 < \lambda < 10$ cm, $\theta = 30°$, $\Delta\theta = 25°$

high coherency

stage IV

steepening short-crested gravity waves

$10 < \lambda < 20$ cm, $\theta \approx 15°$, $\Delta\theta = 40°$

decreasing coherency

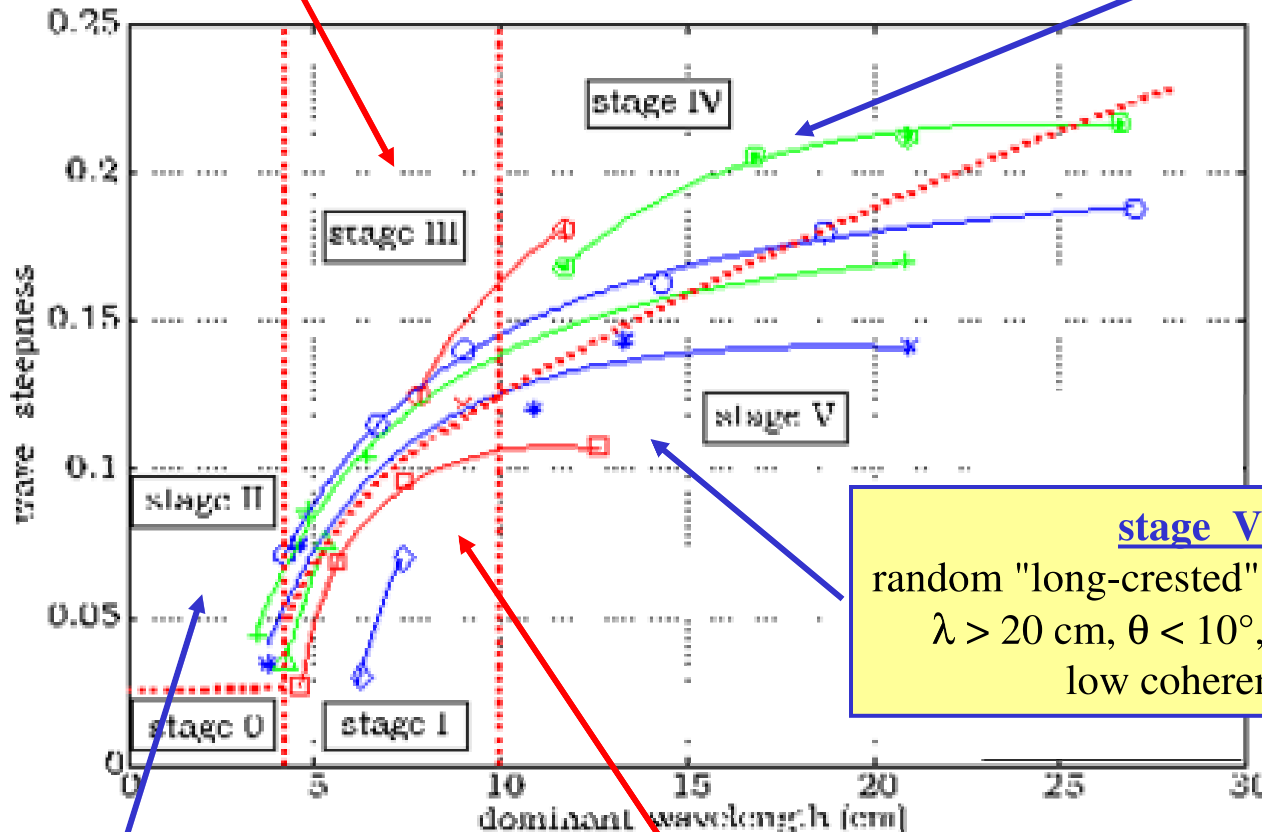

stage V

random "long-crested" gravity waves

$\lambda > 20$ cm, $\theta < 10°$, $\Delta\theta \approx 40°$

low coherency

stage II

short capillary-gravity waves of rough aspect

$\lambda < 4$ cm, $\theta \approx 30°$, $\Delta\theta = 40°$

low coherency

stage I

initial smooth capillary-gravity waves

$4 < \lambda < 10$ cm, $\theta = 30°$, $\Delta\theta = 40°$

high coherency

Origin of the rhombic patterns (stages I and III)

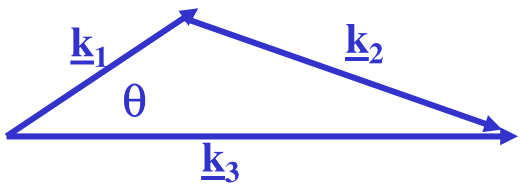

Wilton ripples:

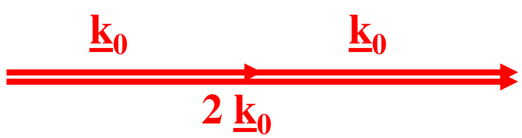

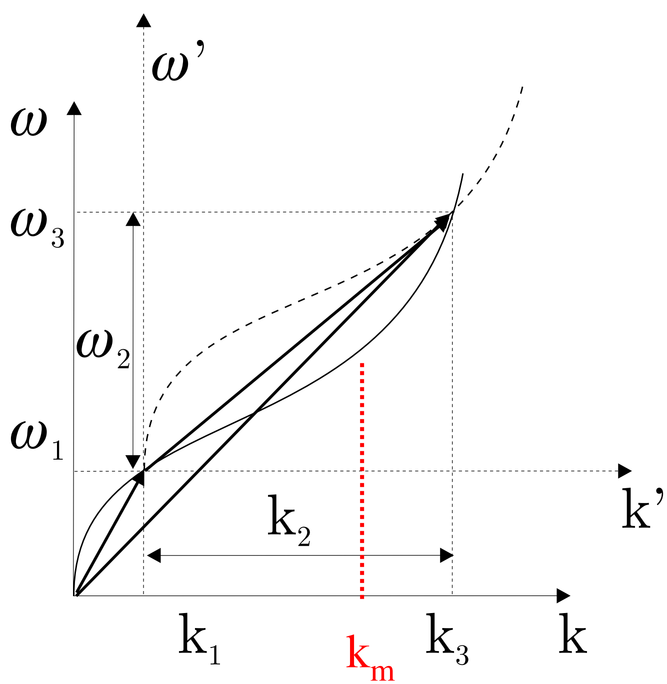

These patterns are observed for capillary-gravity waves of wavelength between about 4 and 10 cm.

3-wave resonant interaction processes ?

$$\underline{\mathbf{k}}_1 + \underline{\mathbf{k}}_2 + \underline{\mathbf{k}}_3 = 0$$

$$\omega_1 + \omega_2 + \omega_3 = 0$$

$$\text{with } \omega_i = c(k_i)\, k_i = g\, k_i + T/\rho\;\; k_i^3$$

$$\theta = 0 \text{ for } k_1 = k_2 = k_0 \text{ (Wilton ripples)}$$

$$\theta \neq 0 \text{ for } k_1 < k_0 \text{ and } k_2 > k_0$$

one difficulty : $c(k_i)$ is dependent on wind speed inducing a shear current in water:

$\Rightarrow$ the minimum value of the dispersion relation is observed at a lower wavenumber k_m:

then, the Wilton ripples are of larger scales:

at 4 m/s, c= 35 cm/s, n_0 = 5.5 Hz, λ_0 = 6 cm

The waves observed are of similar wavelength as the Wilton ripples (Morland, 1993):

$\Rightarrow$ small angles θ ($\theta < 22°$)

The 3-wave resonant interaction process cannot explain the occurrence of rhombic patterns

Horse-shoe patterns (Su et al., 1982)

Instability analysis for gravity waves (Mc Lean, 1982):

1. Modulation instability
due to 4-wave interactions
dominant for ak < 0.30

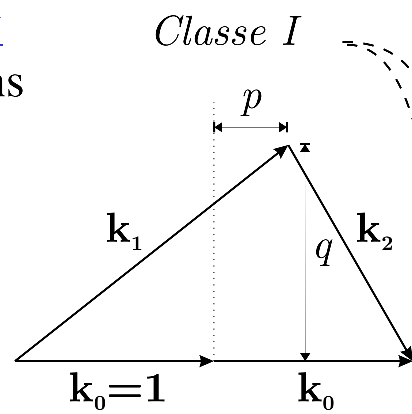

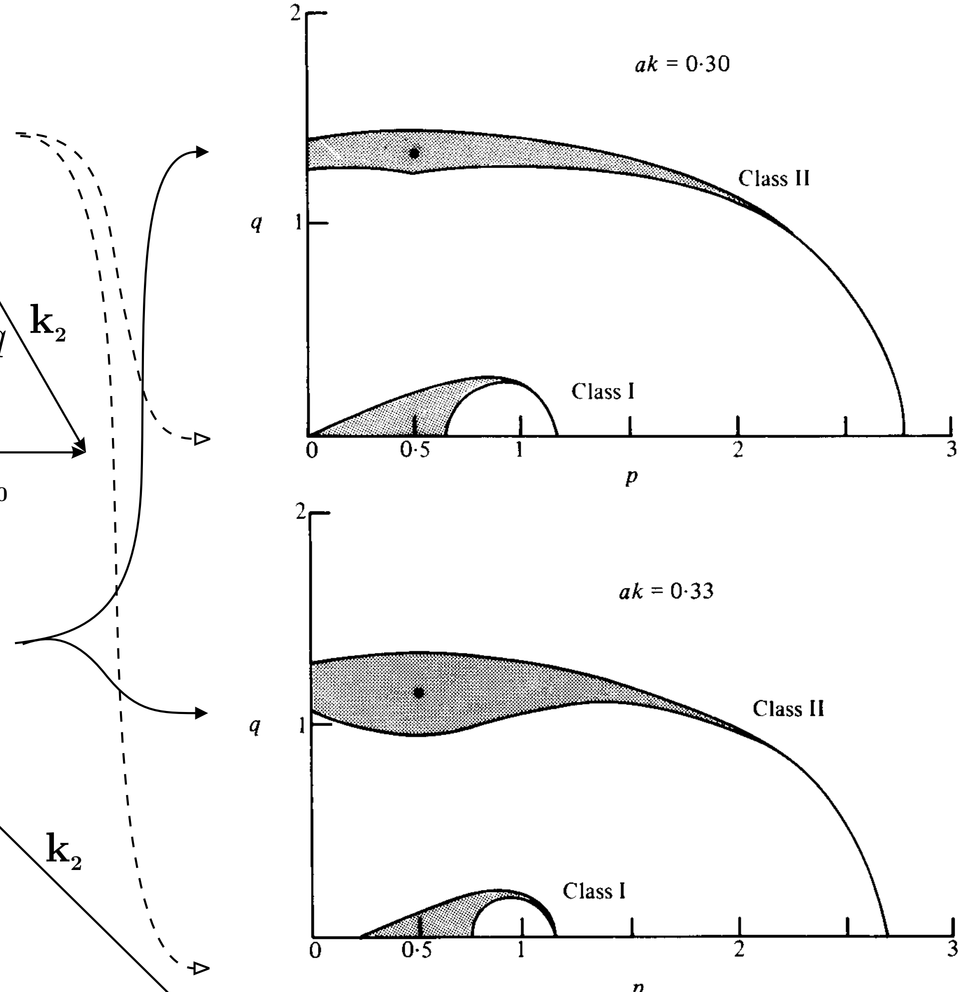

2. Three-dimensional instability
due to 5-wave interactions
dominant for ak > 0.30

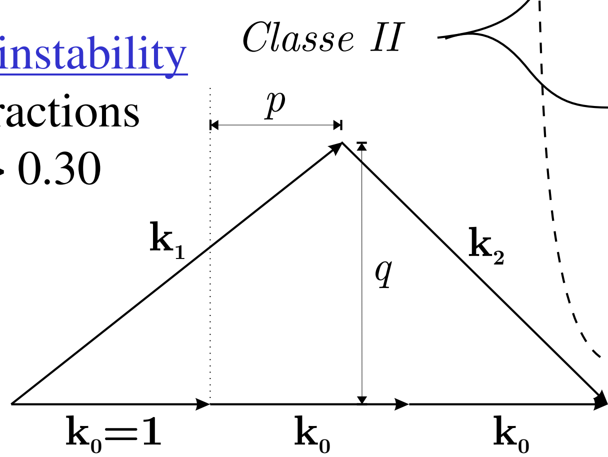

q is dependent on
the basic wave steepness ak

Experimental procedure

The large IRPHE-Luminy wind wave facility

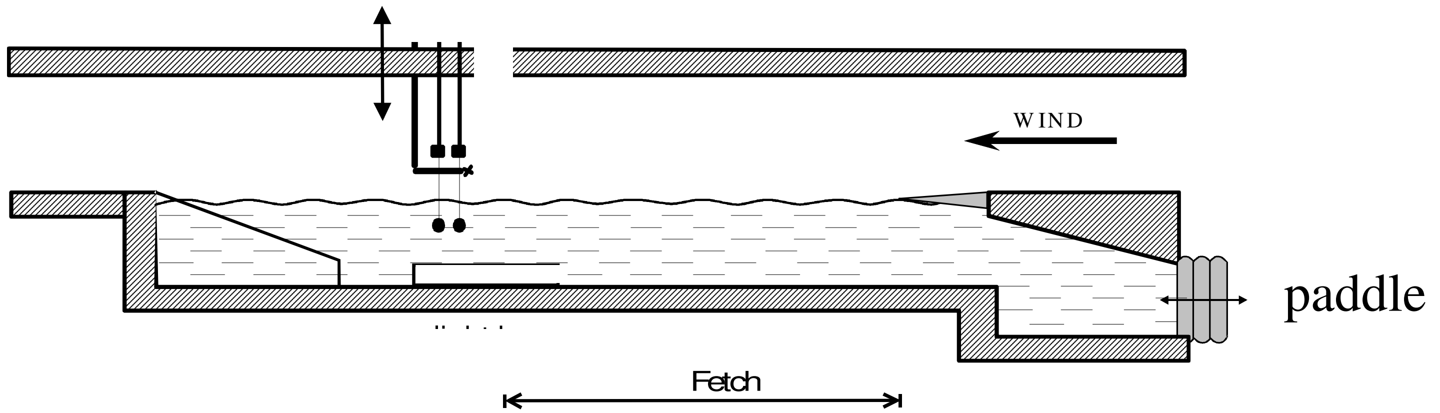

length : L = 40 m ; width : l = 2.6 m ;
water depth : d = 1.0 m ; air tunnel height : h = 1.5 m

The water surface is covered by a long floating plastic sheet damping the modulational instability and acting as a filter of the short wind waves:
$\Rightarrow$ selection of one wave at the wave generator frequency of amplitude increasing with fetch due to wind

Classical horse-shoes patterns

- regular grid of crescents shifted of half-a-wavelength each succesive row;
- steady patterns

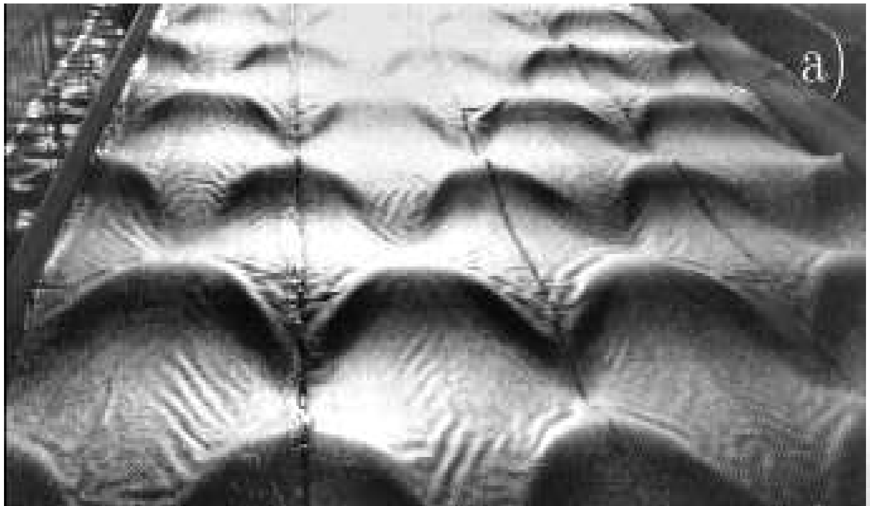

N = 8
f = 1.4 Hz

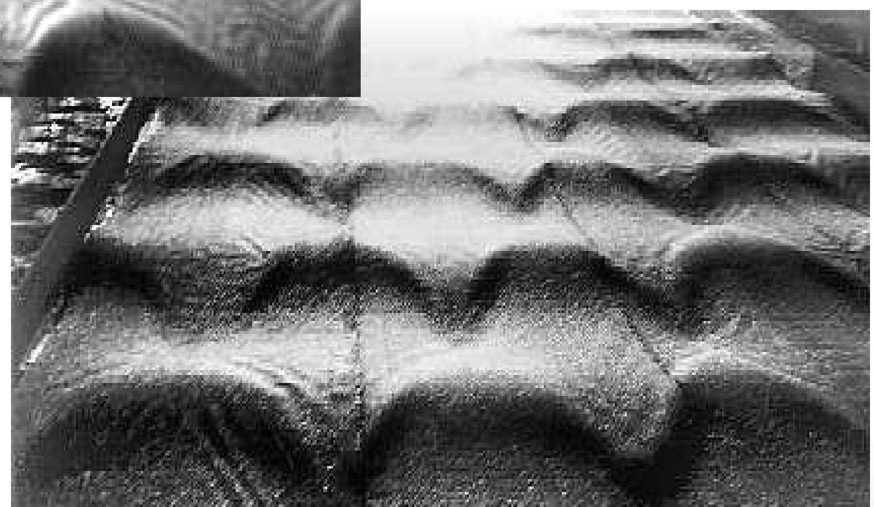

N = 9
f = 1.5 Hz

N = 10
f = 1.6 Hz

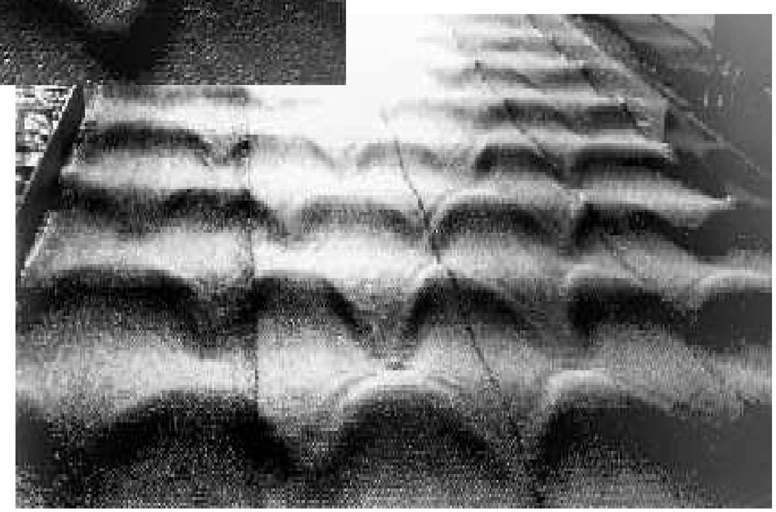

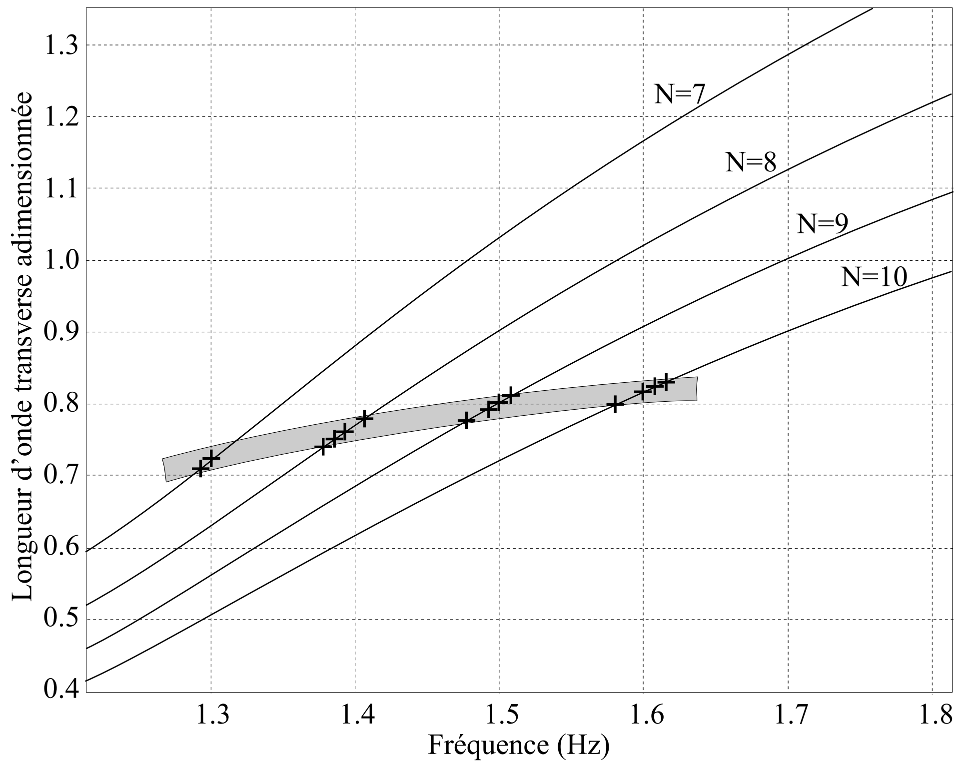

$$\lambda_y = 2\ d\ /\ N$$

N: number of half crosswise wavelength , d: width of the water tank

ak = 0.16 - 0.20

Classical horse-shoe patterns

Oscillating horse-shoe patterns

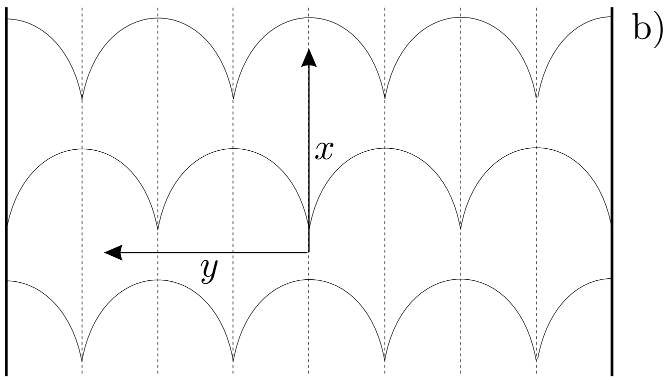

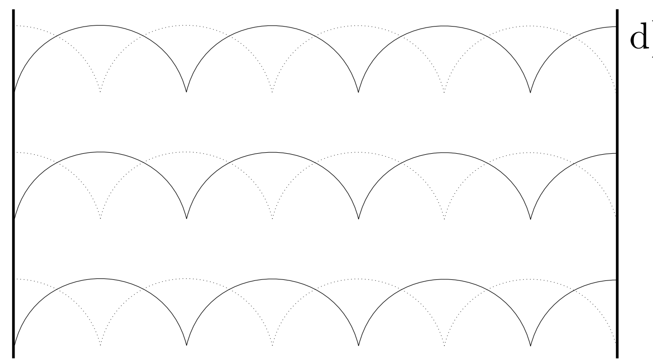

- chess-like crescents
- steady patterns

- crescents aligned in straight rows
- structure oscillating in time with a period of about $3T_o$

Classical horse-shoe patterns

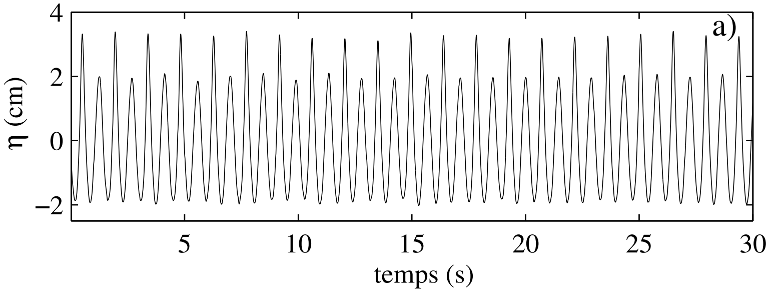

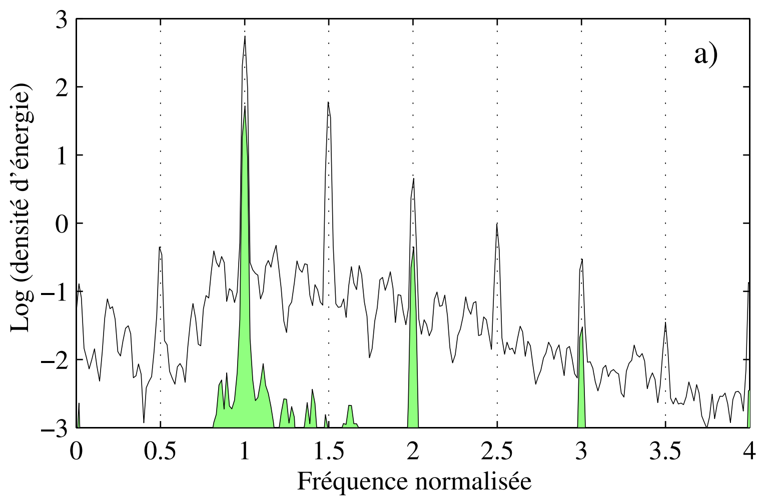

• basic wave: ω_0, $2\omega_0$, $3\omega_0$,...
• 3D disturbances: $\omega_0/2$, $3\omega_0/2$, $5\omega_0/2$,...

Green curve: spectra observed at the entrance of the wave tank (regular sine waves)

Oscillating horse-shoe patterns

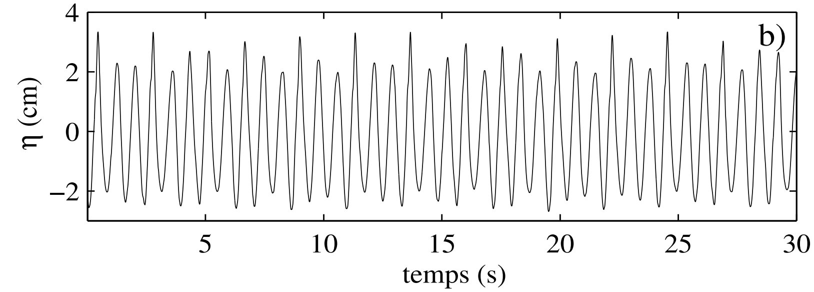

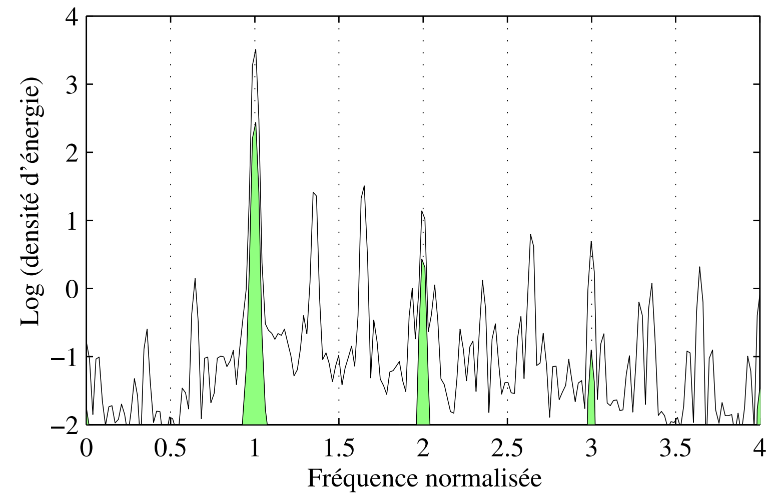

• basic wave: ω_0, $2\omega_0$, $3\omega_0$,...
• 3D disturbances:
$\omega_i = (i+a)\,\omega_0$ and $\omega_i = (i+(1-a))\,\omega_0$
with $a = 0.36$
here: $k_y = 1.32\, k_0$
$k_{1x} = k_0$ and $k_{2x} = 2k_0$

Interpretation of the observations

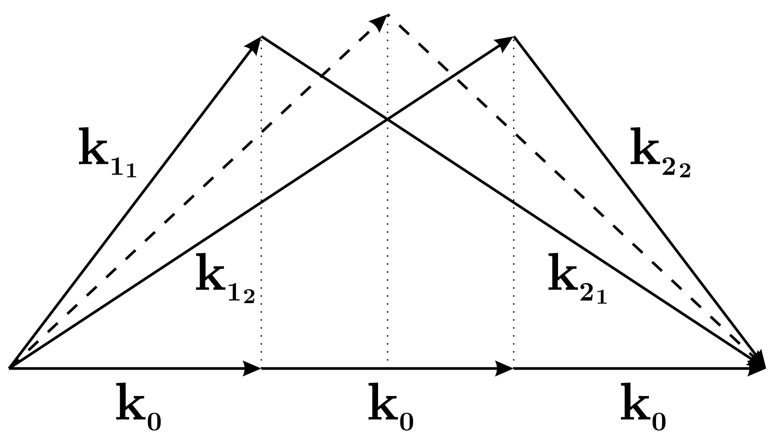

5-wave resonant interaction process

$$\underline{\mathbf{k_1}} + \underline{\mathbf{k_2}} = 3\,\underline{\mathbf{k_0}}$$

$$\omega_1 + \omega_2 = 3\omega_0$$

$$\text{with } \omega_i = c(k_i)\,k_i = g\,k_i + T/\rho\;k_i^3$$

• classical horse-shoe patterns

symmetric quintet configuration

$$\omega_1 = \omega_2 = 3/2\;\omega_0$$

$$k_{1x} = k_{2x} = 3/2\;k_{0x}$$

$$k_{1y} = -\,k_{2y}$$

• oscillating horse-shoe patterns

two-pairs of nonsymmetric quintet configuration

$$k_{1x} = k_{0x} \quad \text{and} \quad k_{2x} = 2k_{0x}$$

$$k_{1x} = 2k_{0x} \quad \text{and} \quad k_{2x} = k_{0x}$$

$$k_{1y} = -\,k_{2y}$$

Conclusions

- existence of coherent patterns for short capillary-gravity waves ($\lambda = 4$-10 cm) due to the existence of two oblique waves propagating at 30° to the wind speed;

- existence of aligned horse-shoe patterns due to 5-wave resonant interaction process with a nonsymmetric configuration.